Faculty of Natural Science and Technology
Department of Physics

NTNU

MASTER'S THESIS
FOR

STUD. TECHN. KRISTIN KARTHUM HANSEN

Project started:	18.10.2008
Project submitted:	13.03.2009

DISCIPLINE: ATMOSPHERIC PHYSICS

Title: *"A study of 1998-2008 Brewer Mk V Spectrophotometer UV-measurements in Oslo."*

This work has been carried out at the Department of Physics, University of Oslo, under the supervision of Professor Arne Dahlback.

Oslo, 13.03.2009

Kristin Karthum Hansen

Abstract

This thesis presents UV data recorded with the Brewer Mk V Spectrophotometer (#042) at Blindern in Oslo. The stability of the instrument is discussed, and a study of the instrument's response from 1998 to 2008 indicates that Brewer #042 has been relatively stable over the last decade. UV Indices obtained from the Brewer measurements are compared to UV Indices obtained with a moderate bandwidth GUV-511 instrument. The 1998 to 2008 mean values for July show that the GUV measurements are on average ca. 7% higher than the Brewer measurements. For the year 2008, UV Indices obtained on clear sky days also indicate that the GUV measurements are on average ca. 7% higher than the Brewer measurements, whereas UV Indices obtained on overcast days suggest that the GUV measurements are close to 10% higher on average, however, these measurements are considered to be more inexact. Finally, the Brewer instrument, which is equipped with a single-monochromator, is compared to the double-monochromator instrument Bentham DM 150 Spectroradiometer at Østerås. A comparison of spectral UV data show signs of improved stray light performance for the Bentham instrument, especially for higher solar zenith angles. When UV Indices are compared, however, the results obtained for the two instruments at various solar zenith angles, deviate by less than 6% for solar zenith angles up to 71.6^o. This suggests that in spite of a poorer stray light performance, Brewer #042 may well be used for UV Index measurements, even at relatively large solar zenith angles.

Preface

This Master thesis is written as a part of my Master of Technology degree at the Norwegian University of Science and Technology (NTNU). The work has been conducted at the University of Oslo (UiO) from October 2008 to March 2009.

The reader is expected to have background knowledge corresponding to that of a university level science or technology student.

I would like to use this opportunity to thank:

- My supervisor Professor Arne Dahlback (Department of Physics, UiO), Senior Scientist Tove Svendby (NILU/UiO) and my teaching supervisor Professor Berit Kjeldstad (Department of Physics, NTNU) for valuable guidance.
- Bjørn Lybekk for help with data conversion essential to this thesis.
- Volodya Savastiouk for clarification regarding Brewer data processing essential to this thesis.
- Ken Lamb at International Ozone Services Inc. for providing new response files for Brewer #042.
- Friends, family and Bent K.O. for support and happy times.

Contents

List of Figures

List of Tables

Listings

Chapter 1

Introduction

1.1 Background

Ultraviolet (UV) radiation is responsible for adverse environmental and health related effects. Fortunately for life on Earth, the atmosphere's stratospheric ozone layer absorbs much of the damaging UV radiation. What gets through the ozone layer, however, can cause problems such as sunburn and skin cancer, particularly for people who spend a substantial amount of time outdoors.

Few high-quality UV radiation measurements have been undertaken up until the last few decades, meaning that scientists working with these issues were for a long time dependent on radiative transfer models. These models are, however, in many cases insufficient, as they require information which may be difficult to obtain, such as the abundance and altitude distribution of gases in the atmosphere, variations in the amount of aerosols, albedo and cloud cover. Measurements are therefore crucial for the verification and continued improvement of these models, and may of course also be used as a substitute. It is also important to obtain high quality measurements over longer periods of time, such as decades, in order to be able to say something about UV radiation level trends. A trend analysis may for instance be interesting as part of a climate change study.

The decrease in total ozone is observed as a wavelength-dependent increase in UV radiation, and spectral UV radiation measurements require high-precision spectroradiometers to detect possible, even though small, changes at these wavelengths. The challenge is to maintain the sensitivity of the instrument at all wavelengths as the dynamic range of the UV is huge. Most of the instruments available today are complicated, expensive

and need to be well-characterized and -maintained. Specifically, they frequently need to be checked for stability and the measured data must be quality-approved.

1.2 Problem to be Addressed

The Brewer Ozone Spectrophotometer is an instrument used for ground-based measurements of ozone and spectral UV radiation. The purpose of this thesis is to study data obtained with the Brewer instrument located at Blindern in Oslo. This Brewer Spectrophotometer has been in operation since 1990, and its UV time series is one of the longest in Europe. However, time series of these data have not been studied up until now.

The main focus of this thesis is the development of a UV Index time series of the Brewer measurements. The stability of the instrument will be discussed, and the UV Index time series will be compared to measurements obtained from a moderate bandwidth GUV-511 instrument. Parts of the time series will be looked at more closely. Specifically, UV indices obtained during clear sky (cloudless) and overcast weather conditions will be compared, and the effects of measuring the irradiance with a single- versus a double-monochromator instrument, for purposes of studying the UV Index, are discussed.

Throughout most of this thesis, UV radiation levels are presented in terms of the UV Index (short form 'UVI', plural form 'UV indices'). The UV Index is a simple measure of the UV radiation level at the Earth's surface and an indicator of the potential for skin damage. It is a measure that many nonexperts are familiar with, as it is being used to raise public awareness and to alert people about the need to adopt protective measures when exposed to UV radiation.

1.3 Scope

Although the Brewer measurements at Blindern started in 1990, the instrument went through several major modifications up until 1998, and the data obtained from the first 8 years of operation are stored in a variety of different formats and folder structures. In order to keep within the time scope of this thesis, only data from the years 1998 to 2008 have been studied.

The complete data processing of the Brewer Spectrophotometer from raw signal to UV spectra is presented. Recent years' studies have shown that the quality assurance of the

Brewer measurements is much improved when correcting for temperature dependence and cosine error, however, these procedures are cumbersome and require measuring equipment which is not available at Blindern, and therefore these correction factors are considered out of scope.

Mid-winter UV irradiance measurements are complicated by low sun angles, as the signal is close to the noise level of the instruments. In addition, as far as the UV Index is concerned, accurate mid-winter values are generally not considered to be of major interest, as mid-winter biological effects due to UV radiation in Oslo are of a negligible order of magnitude. Therefore, detailed investigation of mid-winter measurements is also considered out of scope.

Whenever model calculations (using the radiative transfer model `uvspec`) of the UV spectra and UV indices have been compared to measurements in this thesis, the model calculations have been performed using input parameters which model UV irradiances on clear sky days only. This is because the parameters, methods and uncertainties involved when attempting to compare model and measurements for overcast days are vastly more complex, and considered out of scope.

1.4 Outline

The following chapter will give the reader background theory on UV radiation as well as an introduction to the theory concerning radiative transfer in the atmosphere and information on how ozone and UV radiation are measured. Chapter 3 presents the instruments from which data used in this thesis were obtained and the radiative transfer model `uvspec`. In Chapter 4, the method which has been used to process the Brewer Spectrophotometer data from raw signal to UV Indices is presented, together with the Matlab programs created for use in this thesis and the procedures used to select clear sky and overcast days. The results obtained in this thesis, together with a discussion of these results, are presented in Chapter 5, and finally, Chapter 6 covers the concluding remarks for this thesis.

Chapter 2

Background Theory

In this chapter, background theory on UV radiation, the importance of ozone, as well as biological effects of UV radiation, is presented. This is followed by an explanation of the UV Index and factors influencing UV radiation levels. The concept of radiative transfer in the atmosphere is also introduced, together with a brief description of radiative transfer codes. Finally, various types of methods being used for UV measurements are presented.

2.1 Terminology

Most concepts and definitions will be explained during the course of this thesis. However, the following two definitions, which are SI units, are worth mentioning here:

- **Irradiance (= flux)** [W / m^2]: Describes the power incident on a surface, i.e. the total energy dE (integrated over all solid angles) per unit area dA and unit time dt.

- **Radiance (= intensity)** [W / (m^2·sr)]: Is the irradiance per solid angle $d\hat{\Omega}$.

It is also common to consider each frequency in the spectrum separately. When this is done for radiation incident on a surface, it is called spectral irradiance [W / (m^2· nm)].

2.2 UV Radiation

Ultraviolet light is electromagnetic radiation in the wavelength range from approximately 100 to 400 nm, i.e. shorter than that of visible light, but longer than X-rays. The name means "beyond violet", violet being the color of the shortest wavelengths of visible light. One often divides the UV spectrum into the following 3 types [26]:

UVA	315-400 nm
UVB	280-315 nm
UVC	100-280 nm

The spectrum of the sun's solar radiation is close to that of a black body with a temperature of about 6000 K [28]. UV light forms the high energy component of the solar spectrum, which contains all types of UV radiation when it reaches the top of the Earth's atmosphere. As illustrated in Figure 2.1, a large part of the solar radiation is absorbed by various gases present in the Earth's atmosphere (referred to as absorption bands in the figure). Specifically, one may see that most of the sun's short wavelength UV radiation is filtered out by the ozone (O_3) in the Earth's atmosphere.

2.2.1 Ozone

The gases in the atmosphere absorb the various wavelengths unevenly. O_2 and single oxygen atoms high up in the atmosphere absorb short wave UV radiation. Ozone is important when it comes to the absorption of UVC- and a large part of the UVB radiation. As it turns out, nearly all radiation of wavelength shorter than ca. 295 nm is absorbed before it reaches the ground [12][1].

Ozone is a gas that occurs throughout most of the Earth's atmosphere. It may be "good" or "bad" for people's health and for the environment, depending on its location in the atmosphere. In the troposphere, the air closest to the Earth's surface, ground level ozone is a pollutant which poses a significant health risk. It damages crops, trees and other vegetation and may harm the respiratory systems of animals [39].

The major interest in ozone as an environmental topic, however, owes to the fact that ozone absorbs parts of the UV radiation from the sun. More than 90% of the Earth's

[1] In the wintertime in Norway, radiation of wavelength shorter than 305 nm rarely reaches the ground, as the radiation then passes through a longer path in the atmosphere (due to a lower sun), allowing for more of it to be absorbed.

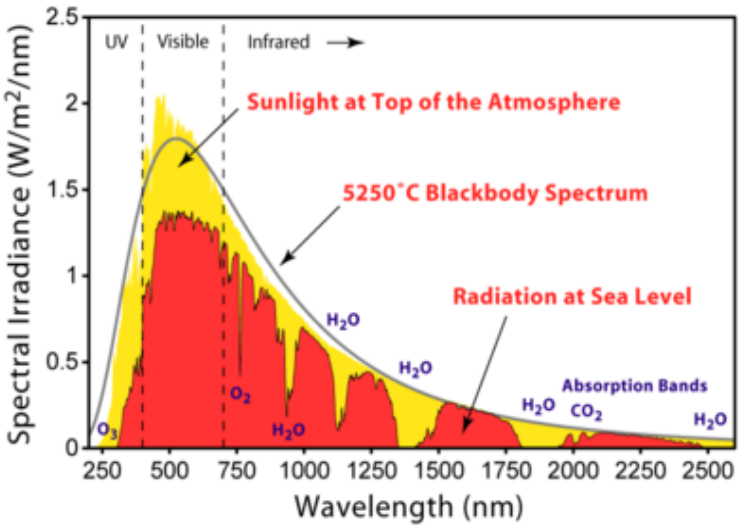

Figure 2.1: Spectrum of the sun's solar radiation. The solar radiation spectrum at the top of the atmosphere is shown in yellow, the solid line represents a blackbody spectrum at 5250°C and the radiation reaching the earth surface at sea level is shown in red. The UV, visible and infrared regions of the spectrum are also indicated. Taken from [40].

ozone is found at altitudes between 12 and 30 km, in the Earth's stratosphere. This is where the so-called *ozone layer* is located. Without the ozone layer, 30-40 times more UV radiation would be measured at ground level, which would imply major consequences for life on Earth [12]. Information on the creation and destruction of ozone, as well as the processes involved when ozone absorbs UV radiation, may be found in [28].

The Dobson Unit (DU) is used to express the concentration of ozone in the Earth's atmosphere over a specified area. One imagines all the ozone in a column reaching from an area on the Earth's surface to the top of the atmosphere being concentrated in a single layer of pure ozone at a temperature of 0^oC and a pressure of 1 standard atmosphere. One Dobson unit then refers to a layer of ozone that would be 10 μm thick [28]. For example, 300 DU of ozone, which is a typical value for atmospheric ozone levels, would occupy a layer only 3 mm thick.

2.2.2 Biological Effects

UV radiation presents both harmful and beneficial effects on human beings. For instance, a positive effect of UVB exposure is that it induces the production of vitamin D in the skin. However, an overexposure to solar UV radiation may result in acute and chronic health effects on the skin, eye, and immune system, such as sunburns, eye damage, skin

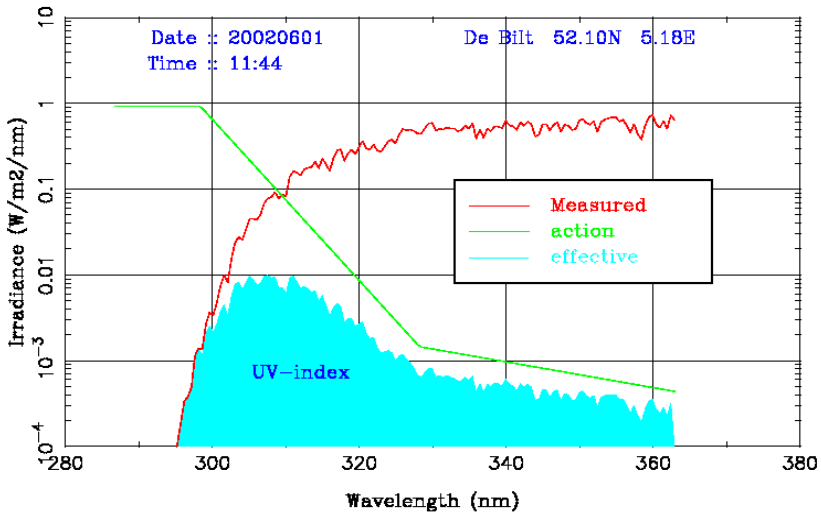

Figure 2.2: In red is shown an example of an ultraviolet spectrum measured on a cloud-free day (measured with the Brewer Spectrophotometer at De Bilt (Netherlands) on 1 June 2002). The CIE erythemal action spectrum is shown in green. The multiplication of these two gives the erythemal UV spectrum (the effective spectrum), and the surface below this graph (shown in yellow), multiplied by 40, is the UV Index. Figure by Marc Allaart, KNMI, De Bilt. Taken from [38].

ageing and skin cancer [26].

The effect that a biological system experiences upon exposure to UV radiation depends upon the wavelength. For instance, a human being will not tan behind a glass window, as the glass absorbs the shorter wavelengths (300-350 nm), which most efficiently tan the skin. The photosynthesis of plants, however, depends upon radiation in the visible range (400-700 nm), and the plants may thus grow behind a glass window (greenhouse). The effects of the UV radiation as a function of the wavelength are described by an *action spectrum*. Every biological effect has its own action spectrum [12].

The CIE eryhtemal action spectrum [24], shown as the green line in Figure 2.2, is a model for the susceptibility of caucasian skin to sunburn (erythema). It may be defined with the following equations:

- $\lambda \leq 298$ nm: $\mathrm{A}(\lambda) = 1.0$
- $298\ \mathrm{nm} < \lambda \leq 328\ \mathrm{nm}$: $\mathrm{A}(\lambda) = e^{0.2164(298-\lambda)}$
- $328\ \mathrm{nm} < \lambda \leq 400\ \mathrm{nm}$: $\mathrm{A}(\lambda) = e^{0.0345(139-\lambda)}$
- $\lambda > 400$ nm: $\mathrm{A}(\lambda) = 0.0$

The CIE action spectrum depicts UVB as much more damaging for human beings when it comes to sunburn than UVA. However, as nearly all UVC and approximately 90% of UVB radiation is absorbed by the atmosphere, the UV radiation reaching the Earth's surface is largely composed of UVA with a small UVB component. This may be seen as the red line in Figure 2.2. Hence, the effective spectrum

$$E(\lambda) = A(\lambda) \cdot I(\lambda), \tag{2.1}$$

where $A(\lambda)$ is the CIE action spectrum and $I(\lambda)$ the measured irradiance, becomes most damaging between 300 and 320 nm, as shown in turquoise in Figure 2.2.

2.2.3 The UV Index

The UV Index (UVI) [26] is a dimensionless quantity used to forecast the likeliness of skin damage caused by UV radiation from the sun, at a particular time in a particular place. A dose rate D can be defined as an integration over the effective spectrum:

$$D = \int A(\lambda) \cdot I(\lambda) d\lambda \tag{2.2}$$

The UV Index is defined as the erythemal UV dose rate D (in $\mathrm{W/m^2}$) multiplied by 40 $\mathrm{m^2/W}$:

$$UVI = 40 \cdot D = 40 \cdot \int_{290}^{400} A(\lambda) \cdot I(\lambda) d\lambda. \tag{2.3}$$

The measured irradiance used in UV Index calculations is the sum of direct beam irradiance and the downward component of diffuse irradiance. Direct irradiance is the sunlight received directly from the sun. Diffuse irradiance is sunlight received indirectly as a result of scattering due to atmospheric constituents (e.g. clouds, aerosols and gas molecules)[2], or other obstructions in the atmosphere or on the ground.

The main purpose of the UV Index is to provide the public with an easy-to-understand daily forecast of the UV irradiance, in order to effectively help people protect themselves

[2]Scattering due to gas molecules in the atmosphere is called Rayleigh scattering, which is inversely proportional to the fourth power of the wavelength, meaning that the shorter wavelength of blue light will scatter more than the longer wavelengths of green and red light. This gives the sky a blue appearance. Scattering due to clouds and aerosols is primarily Mie scattering, which is not wavelength dependent, explaining why clouds appear white after sun light has passed through them.

Table 2.1: UV Index, exposure levels and precautionary needs for various locations. Taken from [37].

UV Index	≤2	3-5	6-7	8-10	≥11
Exposure level	Low	Moderate	High	Very High	Extreme
Precautions	No protection necessary	Some protection necessary.		Extra protection necessary.	
Corresponds to	Winter in Norway.	April-May and August-September in Southern Norway. May-August in Northern Norway.	June-July in Southern Norway. May in the high mountains (in Norway).	June-July in the high mountains (in Norway). Summer in the Mediterranean countries.	Areas around the equator. Alpine areas. UV Index 12 is the limit value for solariums.

from the UV light. It is usually given for local solar noon, when the sun is highest in the sky. The index is an open-ended linear scale, with higher values representing higher UV exposures, and therefore a greater risk of damage to the body. The reason for the dose rate to be multiplied by 40 is to obtain more user-friendly numbers in the scale.

An index of 0 corresponds to zero UV radiation, as is essentially the case at nighttime. The highest values are found on mountain tops at low latitudes, where UV Indices between 15 and 20 have been recorded [37]. In the southern parts of Norway, the UV Index may reach about 6-7 in the summer. Table 2.1 lists typical UV Index values for various locations, as well as exposure levels and precautionary needs. A UV Index below 2 indicates that one may safely be outdoors without sun protection. If the UV Index is above 3, the UV radiation may cause immediate effects (such as sunburn), and protection should be used. The protection may include sunscreen with high SPF (sun protection factor), sunglasses, clothing and a hat. If the UV Index is above 6-7, one should seek shade and avoid the sun during midday [34].

2.2.4 Factors Influencing UV Radiation Levels

The sensitivity of surface UV amounts to a number of physical factors, such as the sun's elevation, latitude, altitude, ozone, surface albedo, clouds and aerosols.

The Sun's Elevation

The length of the radiation's path through the atmosphere is determined by the solar zenith[3] angle; the smaller the solar zenith angle is (i.e. the higher the sun is in the sky), the shorter the path is, which allows for less scattering and absorbtion by the atoms and molecules in the atmosphere.

Latitude

The mid-day sun is higher in the sky at lower latitudes, meaning that the radiation's path through the atmosphere is shorter. In addition, one finds the greatest ozone column abundances at middle and high latitudes [28]. Thus, more radiation is absorbed and scattered before reaching the Earth's surface at middle and high latitudes, than compared to the equatorial regions.

Altitude

Higher altitudes also imply that the UV radiation passes through a shorter path in the atmosphere. Hence the UV radiation levels increase with increasing altitude.

Ozone

As already mentioned, ozone absorbs parts of the UV spectrum. Ozone levels vary over the year (and may even vary by several tens of DU during a day), and as a consequence, the UV radiation levels measured on Earth may differ correspondingly.

Surface Albedo

The albedo of an object is the extent to which it diffusely reflects light from the sun, and it is therefore a more specific form of the term reflectivity. Albedo is defined as the ratio of diffusely reflected to incident electromagnetic radiation. It is a unitless measure, and the range of possible values is from 0 (dark) to 1 (bright). The surface albedo, or ground reflectance, may add to the diffuse radiation to varying extents, e.g. fresh snow can reflect as much as 95% of UV radiation [2] and dry beach sand about 15% [26].

[3]Zenith at a given point is the local vertical direction pointing away from direction of the force of gravity at that location.

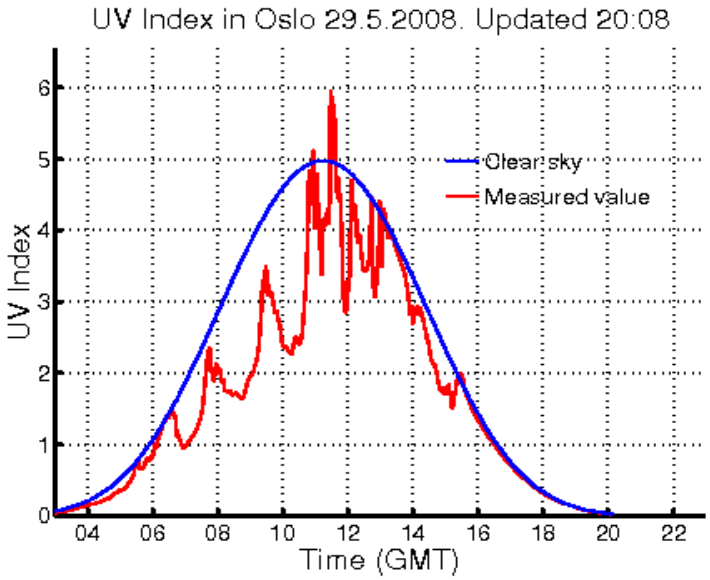

Figure 2.3: The UV Index measured with the GUV-511 instrument at Blindern in Oslo 29. May 2008 is shown in red. The blue line represents the expected UV Index at the same time and location, given clear sky conditions. Taken from [34].

Clouds

A dense cloud cover effectively reduces the UV radiation levels through absorption and scattering in the clouds. Scattered clouds may, however, actually increase the temporary, local UV radiation levels measured at spots that are not left in the shade on the ground beneath the clouds, as the strong forward scattering properties of clouds[4] have much the same effect as the reflectance by different surfaces. An example of this is shown in Figure 2.3, where the measured UV Index is shown in red and a seasonally expected value (given clear sky conditions) is shown in blue. The 'dips' in the red line are probably caused by clouds shielding the instrument from direct solar radiation, whereas the high peaks around noon suggest that scattered clouds are no longer in the path directly between the instrument and the sun; rather, they now contribute to the diffuse radiation, and thus an increased UV Index is measured for a short period of time.

[4]Mie scattering, see [28]

Aerosols

Aerosols are tiny particles (of less than 10 μm in diameter) suspended in the air. They may be produced either naturally, as e.g. dust, sea salt and volcanic debris, or anthropogenically through combustion and industrial processes. Aerosols may affect the radiation field by absorption and scattering, depending on their origin. Further information about aerosols may be found in [28].

2.3 Radiative Transfer in the Atmosphere

The abovementioned factors will cause a beam of radiation moving through the Earth's atmosphere to experience both loss and gain of radiative energy. Loss is due to absorption as well as scattering of radiative energy away from the direction of the beam, and gain takes place as a result of emission by atmospheric constituents or whenever scattered radiation from other beams joins this beam's path.

The effects of these influences may be described mathematically by the radiative transfer equation (RTE). The term radiative transfer refers to the physical phenomena of energy transfer in the form of electromagnetic radiation. RTE simply says that as a beam of radiation travels, it loses energy to the atmosphere by absorption and gains energy by atmospheric emission, and redistributes energy by scattering. The differential form of RTE may be written as:

$$\frac{dL}{\beta ds} = -L + [1-\omega]\, B(T) + \frac{\omega}{4\pi} \int p(\hat{\Omega}, \hat{\Omega}') L(\hat{\Omega}') d\hat{\Omega}', \tag{2.4}$$

where:

- dL is the change in the radiance along a path ds. L is the radiance at the location (x, y, z) and β is the volume extinction (scattering + absorption) coefficient.
- The first term on the right side is proportional to the loss of radiation due to extinction (scattering + absorption).
- The second term is the gain due to thermal emission. ω is the single scattering albedo (the ratio of scattering efficiency to total light extinction), and $B(T)$ is the Planck function (which describes the spectral radiance of electromagnetic radiation at all wavelengths from a black body at temperature T).

- The third term is the gain due to multiple scattering, where $p(\hat{\Omega}, \hat{\Omega}')$ is the phase function giving the likelihood of a scattering event redistributing radiation from direction $\hat{\Omega}'$ to $\hat{\Omega}$.

A thorough examination of the components in and the derivation of this equation is provided in [32]. Analytic solutions to the radiative transfer equation exist for simple cases but for more realistic mediums with complex scattering effects numerical methods are required.

2.3.1 Atmospheric Radiative Transfer Codes

Numerous methods and radiative transfer codes exist to solve the RTE. These codes may be classified according to their solver method, the properties of the atmosphere, the characterization of boundary conditions and the type of output:

- The solver method is based on a numerical discretization of the RTE and a model geometry.
- The properties of the atmosphere may include scattering properties of cloud droplets, ice crystals and aerosols, as well as scattering and absorption properties of air molecules.
- Boundary conditions may be characterized by the albedo and the bidirectional reflectance distribution function, BRDF (which defines how light is reflected at an opaque surface).
- The type of output may for instance be radiance [W / (m^2·sr)] or spectral irradiance [W / (m^2· nm)].

Mainly due to the constraints of computational time, there is no radiative transfer model which is able to answer all possible questions reasonably. Radiative transfer codes are used in a broad range of applications, e.g. related to numerical climate and weather predictions, and different applications require different RTE solvers.

For calculations in a clear (cloudless) sky atmosphere, a one-dimensional radiative transfer model like e.g. DISORT [31] is sufficient. DISORT may also be used to model effects of for instance clouds and aerosols, however, for large solar zenith angles ($>70^o$) one may need to take the sphericity of the Earth into consideration. For this, a pseudo-spherical

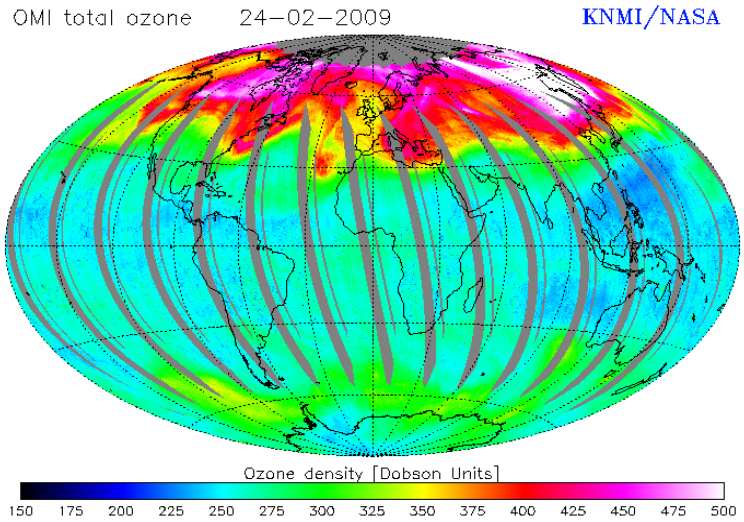

Figure 2.4: Total ozone as measured by OMI (Ozone Monitoring Instrument) onboard the NASA satellite Aura, on 24. February 2009. Taken from [16].

or fully-spherical correction [4] can be used. More complicated situations may include the investigation of two- or three-dimensional effects (for instance inhomogenous surface albedo due to snow cover, or structured, realistic clouds), and special models have been developed to solve a vast amount of applications. Out of all of today's model types, the forward Monte-Carlo model, which traces individual photons through the atmosphere, is probably able to consider the most requirements at the same time.

According to [21], there is general agreement that the RTE can be solved with state-of-the art models to an accuracy of 1% or better. The basic uncertainty is the parameterization of the input data, which ranges from an appropriate description of the atmosphere and the surface albedo, to the extraterrestrial irradiance and its variations.

2.4 Measurements of Ozone and UV Radiation

There are numerous ways to determine the amount of ozone in the atmosphere. Ground and satellite based spectrometers measure ozone by comparing a frequency of the UV spectrum which is strongly absorbed by ozone with one that is not. Measurements can be based on light from the sun, moon, or stars, and different techniques enable measurements to be taken in varying weather conditions and throughout the day. Other techniques include in-situ measurements with weather balloons, air planes or sounding rockets, as well as the LIDAR (Light Detection and Ranging) measurement technique

which relies on the absorption of laser light by ozone.

All ozone measurements before 1978 were undertaken with a ground-based instrument called the Dobson Spectrophotometer, which was designed by Gordon Dobson towards the end of the 1920's [12]. The Dobson instrument measures ultraviolet solar radiation at 2 to 6 different wavelengths from 305 to 345 nm, and calculates the amount of ozone by comparing a frequency which is strongly absorbed by ozone (305 nm) with one that is not (325 nm) [5]. All measurements with the Dobson instrument are manual and relatively time-consuming, and the maintenance requirements of the instrument are rather extensive.

Towards the end of the 1980's, a new type of ground-based instrument, the Brewer Spectrophotometer, was put into service. It measures ozone and spectral intensity profiles of UV radiation, and may operate in a fully-automated mode, which means that it requires much less maintenance than the Dobson instrument. It has become a popular choice of instrument for ground-based measurements worldwide, and other similar instruments have been developed since its introduction.

The GUV-511 and NILU-UV instruments represent a different type of ground-based instruments in use today. They measure UV irradiances in 4-5 channels from which one may model complete UV spectra, and derive the amount of ozone. These instruments are simpler and less expensive than high-wavelength resolution spectroradiometers. They have no moving parts, are easy to calibrate and require little attention, which make them easy to maintain and operate in harsh environments, and increases the possibilitiy for geographic coverage of ground based ozone and UV radiation measurements.

From 1978, one has also measured ozone with satellite based spectrometers, which measure the solar radiation being reflected from Earth [12]. The major advantage with satellites is that one may measure the ozone in numerous locations during one single day (the orbital time of these satellites is ca. 100 minutes), including remote locations where ground measurements are difficult to undertake. However, satellite measurements result in a larger degree of uncertainty, and it is difficult to correct defects that occur in the instruments. Earth Probe TOMS (Total Ozone Mapping Spectrometer), along with OMI (Ozone Monitoring Instrument) onboard AURA, are currently the only NASA spacecraft on orbit specializing in ozone retrieval [35]. TOMS was first launched in the satellite Nimbus 7 in 1978, and has since then been used in several other satellites [12]. The global distribution of ozone, as measured by OMI on 24. February 2009, may be seen in Figure 2.4.

According to [2], ozone may be measured with an uncertainty of 1-2%, whereas spectral

global irradiance in the UV is difficult to measure within an uncertainty of ca. 5%, even for the best instruments available today. This is due to a number of sources of error associated with the measurements, some of which will be described in more detail in the next chapter.

Chapter 3

Instruments

The instruments from which the UV and ozone data used in this thesis were obtained, are presented in this chapter. They include the Brewer Mk V Spectrophotometer and the GUV-511 instrument, as well as a Bentham DM 150 Spectroradiometer. The Brewer and GUV instruments are both located at the Blindern campus of the University in Oslo, whereas the Bentham instrument is located at the Norwegian Radiation Protection Authority's premises at Østerås, a few kilometers West of Oslo. Towards the end of this chapter, a description of the radiative transfer model `uvspec`, from which model spectra of the UV irradiance have been obtained, is also provided.

3.1 Brewer Mk V Spectrophotometer

The Brewer Spectrophotometer is an optical instrument designed to measure ground-level intensities of attenuated solar radiation in either the UV or the visible spectral regions. It may provide near simultaneous observations of the total ozone column, the total sulphur dioxide column, the total nitrogen dioxide column and UV spectra [14].

Originally, the Brewer instrument was designed to measure stratospheric ozone, and was intended as a replacement for the Dobson Ozone Spectrophotometer [25]. The instrument was developed in the 1970's by scientists at the University of Toronto and The Atmospheric Environment Service in Canada, and production of the Brewer instrument was started at the beginning of the 1980's, by SCI-TEC Instruments Inc. (today known as Kipp & Zonen Inc.) in Canada. The main Brewers in use today are Mk II, Mk III and Mk IV, of which Mk II and IV are equipped with single-monochromators, whereas

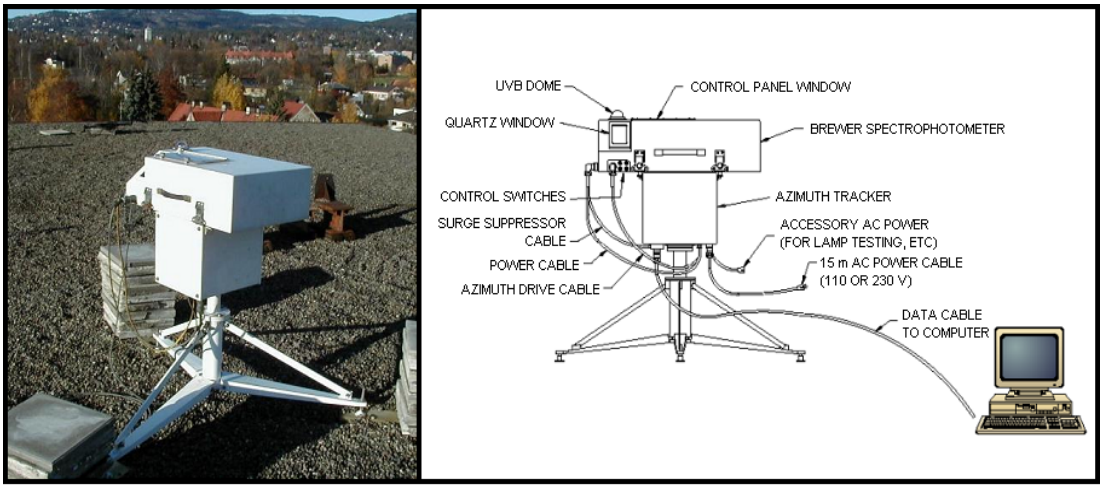

Figure 3.1: (a) Brewer # 042, located on the roof of the Chemistry Building at Blindern. Taken from [34]. (b) A Brewer system. Taken from [7].

Mk III is equipped with a double-monochromator[1].

The Brewer Spectrophotometer located at Blindern has been in operation since 1990, and its serial number is 042. Originally, it measured spectral intensity profiles in the 290 - 325 nm range. It was altered to start measuring in the 290 - 340 nm range in 1995, and in 1998 in the 286.5 - 372 nm range, after which it has been referred to as an Mk V Brewer [2]. Only a couple of Brewers worldwide measure in this extended wavelength range. Figure 3.1 shows Brewer #042, located on the roof of the Chemistry Building at the University in Oslo, as well as a sketch of a Brewer system.

The complete Brewer system is comprised of a spectrophotometer, a solar tracking system and computer equipment running Brewer control and data logging software. A top view of the Brewer mechanical assembly is shown in Figure 3.2. A spectrophotometer is an instrument which splits electromagnetic radiation into components of separate wavelengths, and measures these. The construction may roughly be divided into four parts: the input optics (also known as foreoptics), the wavelength selector (or monochromator), the output optics, and a detector unit. Following is a brief description of the major mechanical, optical and electronic assemblies which make up the basic instrument. A more complete description is provided in [14].

[1]The difference between single- and double-monochromators is further explained in Section 3.3.

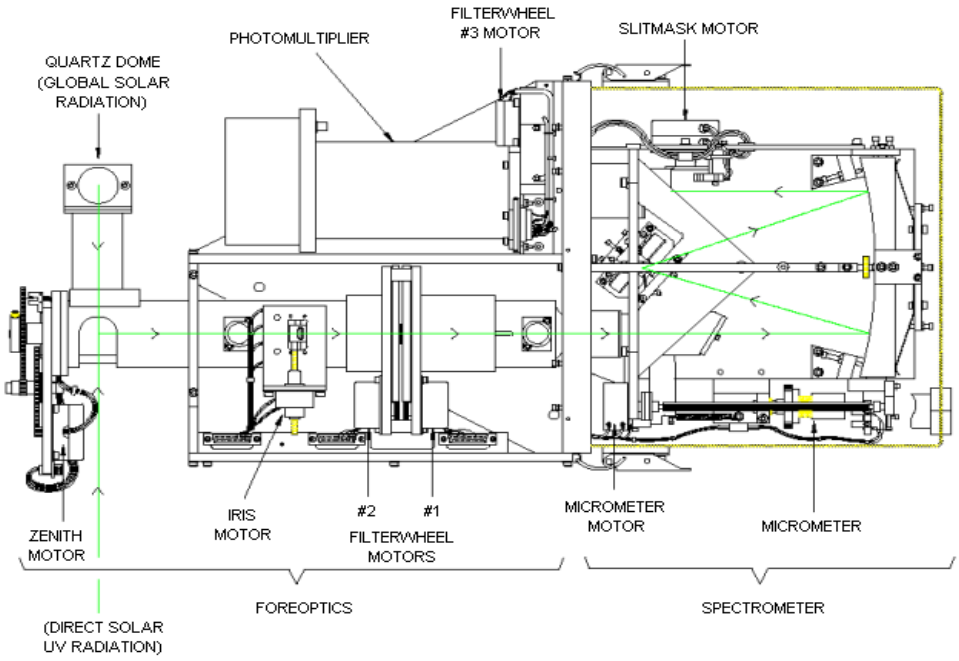

Figure 3.2: Brewer mechanical assembly (top view). Taken (and partially modified) from [7].

3.1.1 Input Optics

When light enters the instrument, it is captured by a prism which may be rotated into several positions in order to capture light from four different sources; the solar zenith light, the direct sunlight, the global solar radiation and the light from two internal calibration lamps. The global solar radiation enters the instrument through a teflon diffusor located at the top of the instrument, protected by a quartz dome, whereas the solar zenith light and the direct sunlight enters the instrument through a quartz window in the instrument casing. All of the optical elements that transmit radiation are made of quartz, because quartz, as opposed e.g. glass, transmits UV radiation.

After the light has been reflected in the prism, it passes through a focusing lens. An iris diaphragm located in the focal plane of the lens limits the field of view of the instrument. After the iris diaphragm, the light passes through a lens which collects the light into a parallel beam of rays, before it passes through two filter wheels, which may be used in different positions. The instrument usually tests the irradiance before every ozone observation and applies an appropriate filter. Further on, the light goes through a polarization filter, whose purpose is to reduce the influence of clouds on

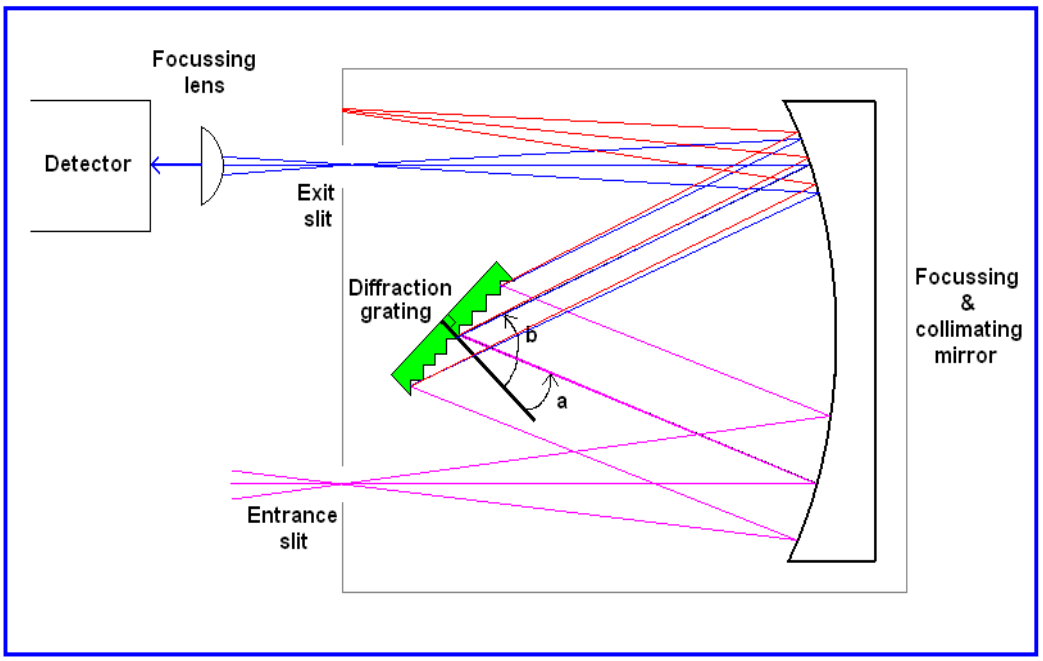

Figure 3.3: Schematic of an Ebert-Fastie monochromator.

ozone measurements conducted with zenith light as the source[2]. Finally, the light passes through another lens and is focused on the entrance slit of the wavelength selector.

3.1.2 Monochromator

The wavelength selector in the Brewer instrument is a monochromator, which splits the radiation into separate wavelengths. The monochromator is a modified Ebert-Fastie configuration, and a typical Ebert-Fastie design is shown in Figure 3.3. The monochromator in the Brewer instrument consists of an entrance slit, a large curved mirror, a diffraction grating and six exit slits (as opposed to the *one* exit slit seen in Figure 3.3). In the Brewer Spectrophotometer there is also a correction lens between the entrance slit and the mirror, and a slit mask with five openings in front of the exit slits. By placing the slit mask in different positions it may be used to block all but one of the exit slits.

[2]This has to do with the fact that radiation measured during clear sky conditions is strongly polarized, because it is mainly Rayleigh scattered (i.e. the light is elastically scattered by particles much smaller than the wavelength of the light), whereas a cloud would act as a depolarizer. The filter does not let through light with the direction of polarization which is dominant for light which has been Rayleigh scattered. Consequently, the influence of the clouds are reduced, because the instrument always "believes" that the weather conditions are cloudy.

The light is dispersed by the diffraction grating. The dispersion is based on Fraunhofer diffraction [11], and may be described mathematically with the grating equation:

$$\sin a + \sin b = K \cdot n \cdot \lambda, \tag{3.1}$$

where a is the angle of incidence and b is the angle of diffraction (both indicated in Figure 3.3), K is the diffraction order, n is the line density of the grating and λ is the wavelength. The grating is operated in the third order for UV and ozone measurements, i.e. $K = 3$. The grating constant is 1200, which means that the grating has 1200 lines per mm. When K and n are constant, the diffraction angle will be a function of the wavelength.

For ozone measurements, only 5 wavelengths are measured (306.3 nm, 310.1 nm, 313.5 nm, 316.8 nm and 320.1 nm), which means that the grating can be kept in the same position while the mask lets light through one slit at a time. For UV measurements it is more common to measure a spectrum of wavelengths (for the Mk V from 286.5 to 372 nm), at every 0.5 nm. Such a series of measurements is usually called a scan. In these measurements, only one slit is in use, while the grating is rotated so that a and b are changed. This causes the wavelength passing through the exit slit to change.

An ideal spectrophotometer would only measure monochromatic radiation, i.e. radiation of one single wavelength at a time. However, even the best instruments will let a narrow wavelength band through the exit slit. The shape of this band is described by the slit function. This function describes the probability of a photon of a certain wavelength to pass through the exit slit as a function of the nominal wavelength. The width of this band is described by the *Full Width at Half Maximum* (FWHM)[3]. The slit function of the instrument depends on the slit widths, the type of grating, aberrations[4] and the quality of the construction of the system. For Brewer #042 the bandwidth is approximately 0.6 nm [25].

3.1.3 Output Optics

As shown in Figure 3.3, a lens which focuses the light from the exit slits onto the detector is located after the exit slits. Between this lens and the detector, another filter wheel,

[3]The *Full Width at Half Maximum*, or FWHM, is the distance between the wavelengths at the points where there is a 50% probability of the photons passing through the exit slit.

[4]Aberration is a collective name for several effects which may cause the radiation focused by the mirror to form blurred images on the exit slits.

which contains two filters that remove radiation from outside the wanted wavelength range, is located. The ability to remove radiation from outside the wanted wavelength range is one of the most important qualities of the instrument [25]. The unwanted radiation may be either light of other orders or stray light:

- Light of other orders is usually diffracted by the grating. From the grating equation, one may see that when light of the 3rd order with a wavelength of 300 nm passes through the monochromator, light of the 1st and the 2nd order, with wavelengths of 900 nm and 450 nm, respectively, may also pass through the monochromator. This light is removed with a cobalt filter. In theory, light of higher orders will also be able to pass through the instrument. However, light diffracted in the 4th order will in this example imply a wavelength of 225 nm (and shorter wavelengths for even higher orders), and radiation of such short wavelengths is absorbed in the atmosphere.

- Stray light will always pass through a monochromator. Stray light is unwanted radiation which enters the detector together with the radiation one wishes to measure. It may come about as a consequence of reflections and unwanted scattering inside the instrument, and can have a completely different wavelength than the one the monochromator is set at. Stray light may particularly have noticeable effects when the source is relatively weak, or when the transmission through the instrument is low or the detector sensitivity is low. A nickel sulphate filter is used for the removal of as much stray light as possible.

3.1.4 Detector Unit

The detector in the Brewer instrument is a photomultiplier. It registers photons hitting the sensitive area of the detector called the photoelectric cathode. When a photon is absorbed by the cathode, there is a certain probability that an electron will be generated. The electron is accelerated by an electric field in the photomultiplier, and will collide with a series of dynodes. At every collision, several electrons are generated, which finally form an electric pulse at the output of the photomultiplier. The number of pulses is transferred to the computer. Before the irradiance may be calculated from this number of counts, one has to correct for the dark current and the dead time:

- Dark current comes from pulses that are created when thermally generated electrons are created in the cathode. One way to reduce the dark current is to cool

down the detector, however, this is not done in the Brewer instrument. Rather, the dark current is measured before each observation, by keeping the slit mask in a position where all of the exit slits are blocked, and later subtracted from the observed values.

- Dead time is the amount of time it takes from one photon is detected until the photomultiplier is ready to detect a new photon. If two photons, which would normally generate one pulse each, enter the detector with a time difference smaller than the dead time, this will be counted as one pulse. Due to this, the photomultiplier is not linear, as the probability of a photon not being counted increases with increased light intensity. The radiation is assumed to be Poisson-distributed [25], which makes it possible to correct for dead time and calculate the correct number of photons per second based on the detected number of counts.

3.1.5 Instrument Box

The Brewer is designed for continuous outdoor operation. It is therefore housed in a durable weatherproof shell which protects the internal components, and enables the instrument to operate reliably and accurately over a wide range of ambient temperature and humidity conditions [14]. In addition to the spectrometer, the electronics that control the instrument and the power supply, are located inside this instrument box. The instrument box is mounted on an azimuth positioning system, also known as an azimuth tracker, which aligns the instrument towards the sun throughout the entire day.

3.1.6 Maintenance and Calibration

For the interior of the instrument to stay dry, two containers filled with silica gel are placed inside the instrument box. The silica gel absorbs moisture, and needs to be replaced every 2-3 weeks. Regular maintenance of Brewer #042 also includes rinsing the quartz dome and window a couple of times per week.

In order to be able to calculate the spectral irradiance, the response of the instrument needs to be known, i.e. the instrument must be calibrated. When the instrument is compared to a known reference, one may determine the connection between the number of counts per second and the irradiance, for each wavelength.

Once a year, usually in June, a representative from International Ozone Services Inc. [17] provides calibration services to Brewer #042 in Oslo. The instrument is compared to

a Brewer travelling standard instrument (#017), and checked for stability, performance and software updates. The spectral response of the instrument is also measured, and stored in a *response file*. The response of the instrument may be found using two different methods. In the first method, one compares Brewer to another instrument which has been calibrated. One may for instance use simultaneous measurements of the global irradiance for this comparison. The other method is to measure a light source whose emission is known. Usually, one uses a certified 1000 W lamp [2].

Brewer #042's response files will be further studied in Section 5.1. Details on each year's calibration service may be found in a *Calibration Report*, available upon request from [2].

3.1.7 Brewer Software

The Brewer Spectrophotometer is supplied with a complete set of programs which control all aspects of data collection and some analysis, as well as control routines to make sure that the instrument functions adequately.

The computer is programmed to interact with an operator to control the Brewer in either a manual, a partially automated or a fully-automated mode of operation [14]. In the latter, the instrument executes a specific sequence of routines throughout the whole day, and stores the measured data in a computer. This is the usual mode of operation for Brewer #042 in Oslo, which means that an operator is mainly required for maintenance purposes.

The data collected during each day is stored on the computer's hard disk. The computer program creates one file for each day. For every UV scan, the day, month, year, location, latitude, longitude, temperature in the instrument, average air pressure, integration time, dead time and dark count are stored. For every wavelength, the time (in minutes after midnight), wavelength, grating position and number of counts are stored.

The instrument in Oslo also computes the CIE-weighted UV dose rate, from the measurements obtained in each scan. These dose rates are stored in daily DUV-files (damaging UV). As the instrument only measures irradiance up to 372 nm, a fixed value is used in the computations for the irradiance from 372 to 400 nm. This is assumed to be appropriate as this upper part of the spectrum constitutes a small percentage of the total dose rate.

3.1.8 Brewer Measurement Uncertainties

There are several sources of error and uncertainties associated with measurements of spectral global irradiance in the UV. These include stray light and noise, the stability and calibration of the instrument, wavelength misalignment, spectral resolution and timing errors. The errors associated with the *cosine response* and *temperature dependence* of the Brewer instrument, may also play a significant role in the determination of the total error [19].

Cosine Response

The cosine response characterizes how the response of the instrument varies with the angle of incidence of the direct and diffuse solar beam. The Brewer instrument's cosine response depends on the horizontal teflon diffusor surface located at the top of the instrument, as well as the rotating prism located beneath the diffusor [25]. The spectral irradiance measured by the instrument, may be defined as:

$$F(\lambda) = \frac{d^3E}{dA \cdot dt \cdot d\lambda} \tag{3.2}$$

where d^3E is the net energy of wavelength $d\lambda$, flowing through the surface dA during the time dt. The amount of irradiance which flows through the surface A (i.e. the diffusor), will depend on the cosine of the angle of incidence. The irradiance may therefore be expressed as:

$$F(\lambda) = \int_{2\pi} I(\vartheta, \phi, \lambda) \cdot cos(\vartheta) \cdot d\Omega, \tag{3.3}$$

where $I(\vartheta, \phi, \lambda)$ is the spectral irradiance in the direction of the angle of incidence, ϑ, and the azimuth angle, ϕ, within the solid angle $d\Omega$.

Ideally, the response of all instruments that measure irradiance should be proportional to the cosine of the angle of incidence. In practice, however, available entrance optics differ by more than 10% from the ideal cosine response for incident angles greater than 60^o [29]. Without a correction, this introduces a great uncertainty in the absolute measurement of irradiances, especially when the sun is low.

The procedure required for the determination of the cosine response of the Brewer instrument is relatively extensive, and was for Brewer #042 last performed in 1996 [25].

It is possible to correct for the cosine response [29], however, this is out of scope for this thesis. The correction factor may be calculated for all wavelengths with a model, and will be a function of the ratio of the direct to the diffuse radiation, and information on the solar zenith angle, ozone value and cloud cover is needed.

Temperature Stability

The response of the Brewer instrument is also dependent on the internal temperature of the instrument [19]. According to e.g. [33], the temperature dependence may be attributable to temperature dependencies in the photomultiplier tube and in the filters in front of the photomultiplier. The Brewer instrument is provided with a heating element maintaining the internal temperature above approximately $+8^oC$ under all conditions, however, the instrument is not temperature stabilized.

Correction is applied to the ozone measurements by the Brewer software. For each of the five wavelenghts being measured, a temperature coefficient is provided. Together with the instrument's temperature, which is measured before each ozone observation, a correction factor is calculated for each of the wavelengths. These correction factors are used to correct the count rate before the ozone level is computed. For the UV measurements, however, no correction is applied. According to [18], the temperature correction may vary from -3% to +5% on a summer day at 60^oN, meaning that the temperature dependency may well be worth correcting for.

In order to determine the temperature dependency of the Brewer instrument, one often uses a method where the response is measured in an environment where the temperature may be varied in a controlled manner (e.g. a room or a box). The procedure is rather cumbersome and measuring equipment required for this is not available at Blindern. Therefore, temperature corrections are also considered out of scope for this thesis.

3.2 GUV-511

Throughout most of the analysis in this thesis, the UVI indices obtained from Brewer #042 will be compared to UV indices obtained from the GUV-511 instrument located next to the Brewer at Blindern.

The GUV-511 instrument is designed to measure UV irradiances at 4 channels, with center wavelengths at 305 nm, 320 nm, 340 nm and 380 nm. The instrument only

Figure 3.4: The GUV-511 located at Blindern. Taken from [34].

depends on a working computer and weekly cleaning/inspection, otherwise it is fully automated and very sturdy, with no moving parts. It is temperature stabilized at 40^oC, has a time resolution of 1 minute and a bandwidth of approximately 10 nm FWHM [3]. The instrument is manufactured by Biospherical Instruments Inc., USA [9]. According to [2], there is an uncertainty of approximately 5% in the GUV-511 measurements. Figure 3.4 shows a photo of the GUV-511 located at Blindern.

Using a technique developed by A. Dahlback [3], one may derive complete UV spectra from 290 to 400 nm. When compared to a high-wavelength-resolution spectroradiometer, the relative difference in CIE-weighted UV dose rates for clear sky and solar zenith angles $\leq 80^o$ was $0.6 \pm 1.5\%$ [3]. This suggests a usefulness in comparing data obtained with the GUV-511 instrument at Blindern with data from Brewer #042.

The mid-winter signal, even on a clear sky day, is close to the noise level of the GUV-511 instrument [2], as solar zenith angles at noon are between 80^o and 85^o during the darkest winter months in Oslo. Due to the complications caused by the signal being close to noise level, detailed comparison of mid-winter measurements is considered out of scope.

3.3 Bentham DM 150 Spectroradiometer

In Section 5.6, complete, measured spectra obtained with Brewer #042 have been compared to complete, measured spectra obtained with the Norwegian Radiation Protection Authority's (NRPA) spectroradiometer at Østerås (approximately 6 km West of Blindern).

The spectroradiometer is of the type Bentham DM 150, and is manufactured by Bentham Instruments Inc. It measures spectral irradiance (within 0.8 nm) from 290 to 450 nm. One scan takes approximately 5 minutes, and a new scan is started approximately every tenth minute. The Bentham DM 150 at Østerås is equipped with a double-monochromator, as opposed to Brewer #042, which is equipped with a single-monochromator. In a double-monochromator, two monochromators are connected in series, with their mechanical systems operating in tandem so that they both select the same wavelength. The double-monochromator optical system allows for a much improved stray light performance, and this is especially true for the lower part of the measured UV spectrum [2]. The intercomparison of complete spectra in Section 5.6 will reveal more on this effect.

3.4 The UVSPEC Radiative Transfer Model

In order to obtain UV indices from irradiances measured with Brewer #042, one needs to estimate the 372 to 400 nm part of the spectrum, as UV Index calculations require integration from 290 to 400 nm. The radiative transfer model `uvspec` [23] was chosen for this task. In addition to being used together with Brewer measurements for computations of the upper part of the spectrum, complete `uvspec` model spectra (from 290 to 372 nm) have also been calculated, for comparison with complete Brewer and Bentham spectra in Section 5.6.

`uvspec` is a radiative transfer model which constitutes the central program in the libRadtran library of radiative transfer routines and programs [23]. It was originally designed to calculate spectral irradiances in the UV and visible spectral ranges, but has evolved to become a tool for many applications, including the simulation of instruments, the calculation of the radiation budget of the Earth and the development of remote sensing techniques [22].

Listing 3.1: A simple uvspec input file.

```
                        # Location of atmospheric profile file.
atmosphere_file ../data/atmmod/afglus.dat
                        # Location of the extraterrestrial spectrum.
solar_file ../data/solar_flux/atlas_plus_modtran
wavelength 290.0 290.0   # Wavelength range [nm]
```

3.4.1 RTE Solver

A variety of RTE solvers are implemented in `uvspec`, of which `disort2` is the one chosen for use in this thesis. `disort2` is an improved version of `disort`, which is an implentation of the standard one-dimensional, plane-parallel DISORT algorithm presented in [31]. Plane-parallel solvers neglect the Earth's curvature and assume an atmosphere of parallel homogenous layers. As mentioned in Section 2.3.1, this is generally a good assumption for solar zenith angles smaller than 70^o.

3.4.2 uvspec Input and Output

The input to `uvspec` is specified in an input file. Output is written to `stdout` and can easily be re-directed into an output file:

```
uvspec < input_file > output_file
```

A minimum uvspec input file

An example of a simple `uvspec` input file is seen in Listing 3.1. Comments start with `#`. `atmosphere_file` describes the location of the file containing the vertical profiles of pressure, temperature and optional trace gases, and thus defines the vertical resolution of the atmosphere. `solar_file` identifies the location of the extraterrestrial solar flux file, which defines the spectral resolution. `wavelength` specifies the wavelength range (i.e. a single wavelength in Listing 3.1) for which the calculation will be performed.

Other input values are needed to solve the radiative transfer problem, including solar zenith angle, surface albedo, etc, however, `uvspec` sets default values for these and other variables when they are not specified by the user. One may therefore start with the simple input file presented in Listing 3.1 and modify and extend it to solve the problem at hand, as numerous commands are available to specify the properties of the atmosphere as well as the details for the RTE solver.

Output

The output from `uvspec` consists of one block per wavelength, and the contents of each block depend on what output the user has requested. The input file in Listing 3.1 will produce a single line of output including the wavelength, direct, diffuse down- and upward irradiances and actinic fluxes. These radiation quantities will by default be output at the bottom of the atmosphere.

3.4.3 Input Values Used in this Thesis

In order to obtain the Brewer UV Index, `uvspec` model calculations are used for the simulation of the 372 to 400 nm part of the spectrum. In Section 5.6, complete `uvspec` model spectra (from 290 to 372 nm) have also been calculated, for comparison with complete Brewer and Bentham spectra. In the following, a brief description of the `uvspec` input values used in this thesis is provided. An example of the input files used for the simulation of the upper part of the spectrum, may be seen in Listing 3.2.

- `atmosphere_file`: As mentioned above, `atmosphere_file` describes the location of the atmospheric data file. If no atmosphere file is given, libRadtran will automatically select one of the six standard atmospheres by [1]. Except for in Section 5.4, where the standard atmosphere `afglms` ('Midlatitude Summer') is used, all simulations in this thesis use the U.S. standard atmosphere [36], `afglus`, as recommended by [2].

- `solar_file`: Also mentioned above, `solar_file` identifies the location of the extraterrestrial solar flux file, which defines the spectral resolution. According to [2], `atlas_plus_modtran` is a suitable solar file for this thesis.

- `ozone_column`: As mentioned in Section 2.2.4, the ozone layer may vary by several tens of DU from one day to the next, and it is thus an important parameter to consider when attempting to simulate measured values. The ozone values to be used in the simulation of the upper part of the spectrum will be discussed in Section 4.2, whereas other ozone input to `uvspec` in this thesis has been obtained from Brewer measurements, since these are considered to be quality assured [2]. **??**.

- `albedo`: This input parameter is used to simulate the surface albedo, a number

between 0.0 (default value) and 1.0, which is constant for all wavelengths[5]. The instrument used for ground measurements is situated in a semi-urban environment in Oslo, and according to [2] an appropriate value for this surface albedo is 0.05. This value is used in simulations throughout this thesis.

- `time`: Specifies the time to simulate, in the format year, month, day, hour, minute and second in UTC [6]. For UV Index calculations, one normally uses the irradiance measurements at local solar noon, which during the summertime in Norway is 11 00 00 UTC. `time` is used to correct extraterrestrial irradiance for the sun-Earth distance with the day of year, and in combination with `latitude` and `longitude`, `time` is used to calculate the solar zenith angle. `time` in combination with latitude and longitude is also used to choose a suitable default atmosphere file, if no atmosphere file is specified.

- `latitude` and `longitude`: These are needed to calculate the solar zenith angle, and are for Blindern 59.92 and 10.72 [2], respectively.

- `rte_solver`: As described above, this thesis has used `disort2` as the RTE solver.

- `nstr`: Number of streams used to solve the RTE. The higher the number of streams is, the more scattering directions are considered in the model. However, a large number of streams is generally not a realistic option, due to the consequences for the computational time. Throughout this thesis, `nstr` = 6 has been used, as this was found to be appropriate in [10].

- `wavelength`: The wavelength range for which the calculation will be performed (290 to 400 nm for the ground level UV spectrum).

- `spline`: Spline interpolate[7] between wavelengths input in the first two arguments, in steps of the last argument, in nm.

- `aerosol_default`: Sets up a default aerosol according to [30], with the following properties: rural type aerosol in the boundary layer, background aerosol above 2 km, spring-summer conditions and a visibility of 50 km. The default settings may be modified with a number of other options, two of which are `aerosol_haze`

[5]For wavelength dependent surface albedo, one may use the input value albedo_file, however, the use of this parameter is out of scope for this thesis.

[6]UTC, or Coordinated Universal Time, is a replacement of the former GMT (Greenwich Mean Time) and is 1 hour after Norwegian standard time (2 hours after Norwegian daylight-saving time).

[7]Spline interpolation is a form of interpolation where the interpolant is a special type of piecewise polynomial called a spline.

Listing 3.2: Example of uvspec input file used in this thesis.

```
                          # Location of atmospheric profile file.
atmosphere_file ../data/atmmod/afglus.dat
                          # Location of the extraterrestrial spectrum.
solar_file ../data/solar_flux/atlas_plus_modtran
ozone_column 300.0        # Scale ozone column to this number [DU]
albedo 0.05               # Surface albedo
time 2004 06 07 11 00 00  # Date and time
latitude 59.92            # Latitude
longitude 10.72           # Longitude
rte_solver disort2        # Radiative transfer equation solver
nstr  6                   # Number of streams
wavelength 290.0 400.0    # Wavelength range [nm]
                          # Location of slit function
spline 291 399 1          # Interpolate from first to last in step

quiet
```

and `aerosol_season`. `aerosol_haze` defines the aerosol type in the lower 2 km of the atmosphere, and the user may choose between Rural, Maritime, Urban and Tropospheric type aerosols, as described by [30]. `aerosol_season` is used to specify the season (spring-summer or fall-winter) to get an appropriate aerosol profile.

- `slit_function_file`: If specified, the calculated spectrum is convolved with the function found in the `slit_function_file`. This may be used to better simulate the slit function of an instrument measuring a complete spectrum. In Sections 5.4 and 5.6, a triangular `slit_function_file` is used in the `uvspec` simulations.

Chapter 4

Methods

In this chapter, the methods used to process the data obtained from the ground instruments are explained. As mentioned in Section 3.4, one needs to model the 372 to 400 nm part of the spectrum in order to obtain UV Indices from the Brewer #042 measurements, and the procedure which has been used for this is also described. Finally, the methods used to select clear sky and overcast days are presented.

4.1 Processing Brewer Raw Data

In order to obtain spectra of the irradiance measured with Brewer #042, one needs to convert raw data to count rates, compensate for the dead time, subtract stray light measurements and make use of the response files.

4.1.1 Converting Raw Data to Count Rates

When Brewer #042 measures the irradiance at a specific wavelength, it integrates counts for 0.2294 seconds. This is not always enough time to obtain a sufficient amount of counts. It is not possible to prolong the integration time, hence, the only way to obtain a higher number of counts is to increase the number of integration periods. The integration period is called a "cycle", in the instrument's software. The conversion of the number of counts to a count rate N is done by compensating for the number of cycles, CY and using an interval-scaling factor, IT, which incorporates the integration time as well as the time between each integration. Before each scan, the instrument measures the dark

current in the photomultiplier. The dark count, N_{dark}, is subtracted from the number of counts at each wavelength. Hence, the count rate N becomes:

$$N = \frac{(N_{raw} - N_{dark}) \cdot 2}{CY \cdot IT} \tag{4.1}$$

The count rate is denoted as counts per second in the Brewer Software as well as in the Brewer Manual [14], however, N is actually four times the number of counts per second, because of the number 2 in the above equation and because $IT = 0.1147$, which is the integration time divided by 2.

4.1.2 Compensating for Dead Time

One needs to compensate for the dead time in the photomultiplier. Poisson statistics is assumed for the incoming radiation [14], which implies that for any observation at a true count rate N_0, the observed rate N will be:

$$N = N_0 \cdot e^{-N_0 \cdot DT} \tag{4.2}$$

where DT is the dead time of the photon-counting system. DT is determined by a dead time test which is run as part of the Brewer setup procedures. Eq. 4.2 is solved for N_0 by iterating on the (rearranged) expression:

$$N_0 = N \cdot e^{N_0 \cdot DT} \tag{4.3}$$

4.1.3 Subtracting Stray Light

Although there are filters in the instrument which remove stray light, these are not capable of removing all of the stray light. In order to reduce the problem the remaining stray light is causing, one assumes that all of the irradiance of wavelength shorter than 292 nm is absorbed in the atmosphere. Then the raw counts obtained for wavelengths shorter than 292 nm must be unwanted stray light [25]. The mean value of the number of counts in measurements below 292 nm is therefore calculated, and subtracted from the measurements with larger wavelengths. One assumes the amount of stray light to be equal for all wavelengths. For a scan from 290 nm with wavelength increments of 0.5 nm, the stray light calculated by finding the average of the measurements below 292 nm becomes:

$$N_{stray} = \frac{\sum_{\lambda=290}^{\lambda=291.5} N(\lambda)}{4} \tag{4.4}$$

which means that the number of counts per second is:

$$N_{cps} = N_0 - N_{stray} \tag{4.5}$$

4.1.4 Response Files

As mentioned in Section 3.1.6, calibration services from [17] are provided to Brewer #042 once a year, during which the spectral response of the instrument is measured and stored in a *response file*. The response files contain information about the connection between the number of counts per second and the irradiance, for each wavelength, and the irradiance is determined by dividing the number of counts with the respective response value.

Brewer #042's response files for the years 1998-2008 may be seen in Figure 5.1, and will be discussed in more detail in Section 5.1.

4.2 UVSPEC Modelling of Irradiances from 372 to 400 nm

As mentioned before, one needs to model the 372 to 400 nm part of the UV spectrum in order to obtain UV Indices for the Brewer measurements, and the radiative transfer model `uvspec` was chosen for this task.

Considering a clear sky situation (with normal surface albedo and no aerosols), the main parameters one should expect to influence the irradiance measured in the UV spectrum are the solar zenith angle and the ozone level. In order to determine in what way these two parameters should be included in the `uvspec` input files, the effects of varying them was tested for 'extreme' and normal values at Blindern.

Table 4.1 shows the contribution of the 372-400 nm part of the UV spectrum to the UV Index (the total UV Index is shown in parenthesis), for varying ozone levels and solar zenith angles, as calculated with `uvspec`. Ozone mainly absorbs UVC- and a large part

Table 4.1: Contribution of the 372-400 nm part of the spectrum to the total UV Index, for various ozone levels and solar zenith angles, as calculated with uvspec. The total UV Index is shown in parenthesis.

	Low sun (SZA=83.4)	Medium high sun (SZA=63.0)	High Sun (SZA=36.5)
Low O_3 (200 DU)	0.01 (0.16)	0.07 (2.66)	0.15 (10.95)
Medium O_3 (300 DU)	0.01 (0.12)	0.07 (1.69)	0.15 (6.74)
High O_3 (500 DU)	0.01 (0.09)	0.07 (1.02)	0.15 (3.74)

of the UVB radiation. Thus, the irradiances in the 372-400 nm part of the spectrum (which is completely within the UVA region), should not be affected by varying ozone levels. The results shown in Table 4.1 confirm this theory, as the contribution to the UV Index stays constant for ozone levels varying from very low (200 DU) to very high (500 DU), when, at the same time, the total UV Index is clearly affected. The influence of the solar zenith angle is, on the other hand, evident also at the uppermost wavelengths, with a contribution to the UV Index ranging from 0.01 to 0.15, depending on the solar zenith angle.

Due to the influence of the the solar zenith angle on the uppermost part of the spectrum, it was decided that model spectra would be created for each day in a whole year, so that the seasonal variations of the solar zenith angle at noon could be taken into consideration also for the 372-400 nm part of the spectrum. An example of the type of `uvspec` input files created, may be seen in Listing 3.2. All input parameters, apart from the day number, are kept constant, as `uvspec` uses the input parameter `time` (where day of year is input), in combination with `latitude` and `longitude`, to calculate the solar zenith angle.

4.3 Matlab Programs

With the irradiances sorted out, the UV Index may be calculated according to the method described in Section 2.2.3. The Matlab program which was made to obtain the time series of the UV Index from 1998-2008, `brewerUVItimeSeries.m`, may be seen in Appendix A. This program implements the methods described in Sections 2.2.3, 4.1 and 4.2, and consists of 5 functions which are run for a set of [user input] days in a [user input] year:

- `readResponseFile.m`: As the name indicates, this function takes a [user input] response file as input, reads the information provided in it, and returns the spectral

response[1].

- `readDataFile.m`: This function reads the Brewer data files for the specified days, finds the scan that is closest to noon (11 00 00 UTC, or 660 minutes after midnight) and returns the raw data in this scan. As one scan takes approximately 5 minutes, the scan with the 325 nm measurement closest to noon is selected as the 'noon scan'.

- `processData.m`: This function takes the 'noon scan' raw data as input and returns the data processed according to the methods described in Section 4.1, i.e. the raw data are converted to count rates by compensating for the number of cycles and using the interval scaling factor, the dead time is corrected for and the stray light is subtracted. Finally, a 'processed scan' is returned.

- `calcTailUVI.m`: Here, the contribution of the upper part of the spectrum (nicknamed "tail") to the total UV Index, is calculated.

- `calcUVI.m`: Finally, the total UV Index is calculated. First, the spectral irradiance is computed by dividing the processed data with the respective response value, which allows the contribution of the Brewer measurements to the total UV Index to be calculated. In order to adjust for the fact that clear sky input is being used for the modelling of the upper part of the spectrum, the ratio of the irradiance values measured at the 3 largest wavelengths in the Brewer data file, to the modelled irradiance values at the same wavelengths, is multiplied with the "tail" part of the UV Index. This should adjust for non-static effects caused by e.g. clouds and aerosols. Finally, the total UV Index is returned to `brewerUVItimeSeries.m`.

Parts of the analysis in this thesis will look closer at data obtained from other parts of the day than noon, or at details of the measured spectra rather than the UV Index. The Matlab program `brewerUVItimeSeries.m` has been partially modified in order to obtain the results for these parts of the thesis, however, these modified versions of the program are not included in this thesis. The Matlab programs used to obtain UV Indices from the `uvspec` calculations, as well as the GUV measurements, were presented in [10],

[1] A closer look at this function will reveal that it also returns the largest wavelength ('endWL') read in the response file. The reason for this, is that some of the initial response files provided from [17] did not contain response data up to 372 nm, but rather to 363.5 nm or 370.5 nm. This Matlab program was developed before it was discovered that a new set of response files (all of which contained response data up to 372 nm) could be provided from [17], and this program was therefore made to model the upper part of the spectrum depending on each response file's largest wavelength.

and will neither be included here, as they do not involve the use of any other methods relevant to this thesis, than the ones already presented.

4.4 GUV-511 Measurements

The 1998-2008 time series presented in the next chapter considers the GUV/Brewer UV Index ratios at noon (11:00 UTC). The GUV-511 UV Indices have been obtained from the 'daily summary' data files (available upon request from [2]). These data files contain the CIE-weighted UV dose rates averaged over an hour at noon (in mW/m^2). The UV Indices are then calculated by multiplying the UV dose rate with 0.04.

For the rest of the GUV/Brewer UV Index comparisons in this thesis, GUV measurements obtained at the exact same time as the Brewer scan (i.e. not averaged over an hour at noon) have been used. As one complete Brewer scan takes approximately 5 minutes, and GUV-511 measures the UV Index every minute, the time of the Brewer instrument's 325 nm measurement has been used to select the appropriate minute to use from the GUV-511 measurements.

4.5 Bentham DM 150 Spectroradiometer Measurements

Most of the analysis in this thesis focuses on the study of UV Indices, however, in Section 5.6, Brewer, Bentham and `uvspec` spectra are compared. The Bentham spectra have been obtained from [2]. As the Bentham instrument measures the spectral irradiance approximately every tenth minute, the scans which have been found to be closer to the Brewer scans in time (comparing the time of the 325 nm measurements), have been used in this analysis.

4.6 Selection of Clear Sky and Overcast Days

In Sections 5.4 and 5.5, UV Indices obtained for clear sky and overcast days in 2008 are studied. In Section 5.4, Brewer, GUV and `uvspec` UV Indices will be compared, whereas Brewer and GUV UV Indices are compared in Section 5.5 (`uvspec` simulations of overcast days is considered out of scope).

Listing 4.1: Example of GUV-511 'daily summary' file data.

```
yy  mm dd jul   O3 sig O3  Max D    noon D  Daily dose cld tr. cld opt.
                [DU] [DU] [mW/m**2] [mW/m**2] [J/m**2]  [\%]    depth
2008 5  8 129 350.0  0.3   107.5     106.6     2705      95.7     0.7
2008 5  9 130 348.0  0.2   106.0     103.7     2686      91.3     1.7
2008 5 10 131 350.8  0.2   110.1     108.7     2777      95.8     0.7
2008 5 11 132 347.0  1.6   112.5      81.9     1920      70.2     9.8
```

4.6.1 Criteria for Selecting a Clear Sky Day

The 'daily summary' file of the GUV-511 measurements was examined in order to find a preliminary set of clear sky days in 2008. An example of the type of data provided in this file is seen in Listing (4.1). There is enough useful information in the 'daily summary' file to make a qualified guess as to whether a day is a clear sky day (around noon) or not. The criteria used for selecting clear sky days in this thesis were probably more strict than necessary, in the sense that they reject several days that were in fact clear sky days. However, it was decided that a set of approximately 15 clear sky days would be sufficient for the purposes of this study, and hence there was no need to find *all* of the days in 2008 that would satisfy a meteorologist's or a layman's definition of a clear sky day. For this study, the following criteria were used:

- `cld.tr` $\geq$ 94-95% (The cloud transmission[2] (`cld.tr`), being the ratio of measured 340 nm irradiance to the calculated clear-sky 340 nm irradiance at the same solar zenith angle and at 5% surface albedo, should be greater than 94-95%.)
- `Max D` $\approx$ `noon D` (When the maximum irradiance measured over an hour at noon (`Max D`), and the irradiance averaged over an hour at noon (`noon D`), are of approximately equal values, the cloud situation is likely to have been stable around noon. If, in addition, the cloud transmission is high, either no clouds are present at all, or there is perhaps only a thin, stable layer of cirrus clouds.)
- `sig O3` ≤ 1 (A small standard deviation (`sig O3`) for the ozone also indicates a relatively stable situation around noon.)

Based on these criteria, a preliminary set of approximately 30 days was chosen from the daily summary file. The chosen days are selected from the period between late spring

[2]The cloud transmission describes the effect of cloud cover on the UV radiation. 100% represents clear sky. Clouds will usually lower the UV index. E.g. a cloud transmission of 70% means that the UV index is 70% of the clear sky value.

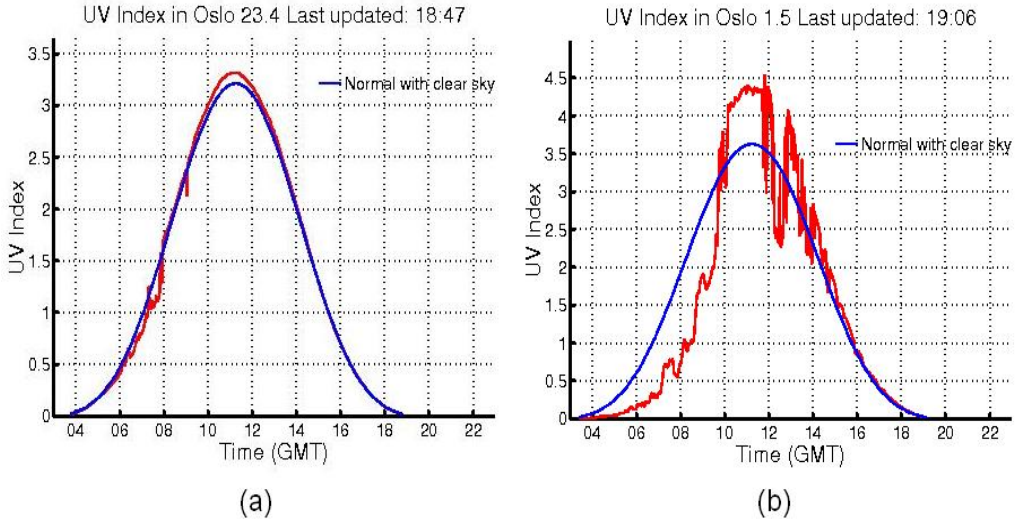

Figure 4.1: Plots of the UV Index as measured with the GUV-511 instrument at Blindern for days (a) 113 and (b) 121 in 2005. (a) appears to be a beautiful clear sky day, whereas (b) is an example of a day that would typically be rejected in the clear sky day selection process, due to the substantial amount of ripples and fluctuations. Taken from [34].

and early autumn, in order to avoid possible effects of snow cover and a high solar zenith angle.

Next, the webpages of the Norwegian Radiation Protection Authority (NRPA) [37], were consulted. Here, full day UV Index plots are provided, and these were studied for the selected days. Figure 4.1 shows two examples of full day UV Index plots[3]. In order for a day to be classified as a clear sky day (in this study), the UV index plot should be rather smooth around noon. Ripples/dips in the plots indicate that clouds (or other obstacles) may have interfered. A number of the days chosen above were rejected in this part of the selection process, and the resulting set of days became: 110, 111, 112, 115, 129, 131, 134, 154, 157, 169, 184, 192, 205, 207, 209, 210, 214, 288 and 291.

4.6.2 Criteria for Selecting an Overcast Day

It is difficult to find stable, overcast weather situations, as cloud layers of varying thickness and density usually drift across the sky, rather than stay put in one location for a

[3]The reason why plots from the webpages of the Department of Physics at the University in Oslo are being used in Figure 4.1, instead of plots from NRPA, is that the plots at the webpages of the Department of Physics are presented in English and that the NRPA plots contain information and data which are not useful here. Both the NRPA and the Departments of Physics plots are created using the same data from the GUV-511 instrument.

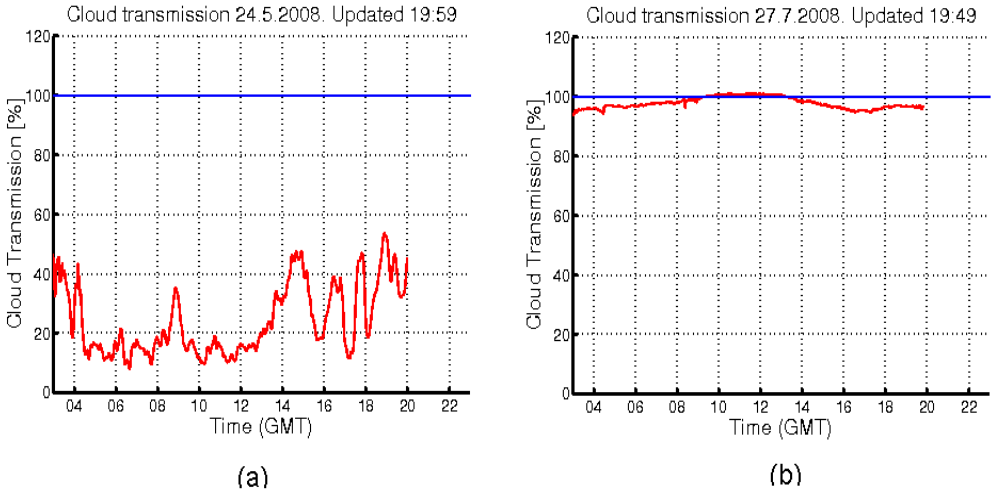

Figure 4.2: Plots of the cloud transmission as measured with the GUV-511 instrument at Blindern for days (a) 145 and (b) 209 in 2008. (a) appears to be an overcast day, with low cloud transmission, whereas the high cloud transmission in (b) suggests that this is a clear sky day. Taken from [34].

longer period of time. Due to this, noon averages of the GUV-511 measurements have not been used in the comparison in Section 5.5.

Figure 4.2a shows the observed cloud transmission measured with the GUV-511 instrument on an overcast day in 2008, whereas Figure 4.2b shows the observed cloud transmission on a clear sky day. Periods of time where a relatively stable cloud transmission of less than ca. 40% could be found to last for at least 20-30 minutes, e.g. as observed in Figure 4.2a from ca. 12:00 to ca. 12:45, have been used in this part of the study. As few observations of this kind were found to take place around noon, observations from other parts of the day, satisfying a solar zenith angle smaller than or equal to ca. 55^o, have also been included. UV Indices obtained from Brewer scans measured during these periods of time have then been compared to the UV Indices obtained from corresponding GUV-511 measurements. The selected GUV-511 measurement is the one taking place at the same time as the 325 nm measurement of the Brewer scan.

The following days, with time of day (UTC) in parenthesis, were selected on the basis of these criteria: 126 (11:09), 136 (12:28), 137 (09:02), 142 (08:55), 145 (12:15), 180 (09:22), 188 (11:01), 189 (15:02), 202 (14:09), 215 (12:45), 220 (12:24), 231 (07:40), 233 (11:47), 239 (09:01), 244 (12:36) and 245 (09:59).

Chapter 5

Results and Discussion

This chapter starts with a presentation of the 1998-2008 response files for Brewer #042. Next, UV Indices obtained from irradiance measurements with the Brewer instrument are presented and discussed. A time series of the ratio GUV-511 to Brewer #042 UV Indices for the years 1998-2008 is provided, and data from the year 2008 is looked at more in-depth. Finally, complete spectra obtained with Brewer #042, the Bentham DM 150 Spectroradiometer and `uvspec`, are compared, and the effects of measuring the irradiance with a single-monochromator instrument, versus a double-monochromator, for purposes of studying the UV Index, are discussed.

5.1 Response Files

During the course of this study, the Brewer #042 response files, which were provided together with each year's calibration report by International Ozone Services Inc. (IOS) [17], were examined. The scanning range of this instrument is up to 372 nm (normal is 363 nm), and this makes the calibration and data processing software difficult to maintain. For other Brewer instruments, it has been common to use a program which has a fitting polynomial to smooth results, however, according to the Brewer #042 calibration report from 1998, this instrument has an unusual increase and then decrease in sensitivity at 350 nm. Therefore, it is assumed to be better to process its response files without using the fitting polynomial to smooth results.

It was discovered that some of the response files initially provided seemed to be improper response files, in the sense that the special fitting polynomial had been applied, or that

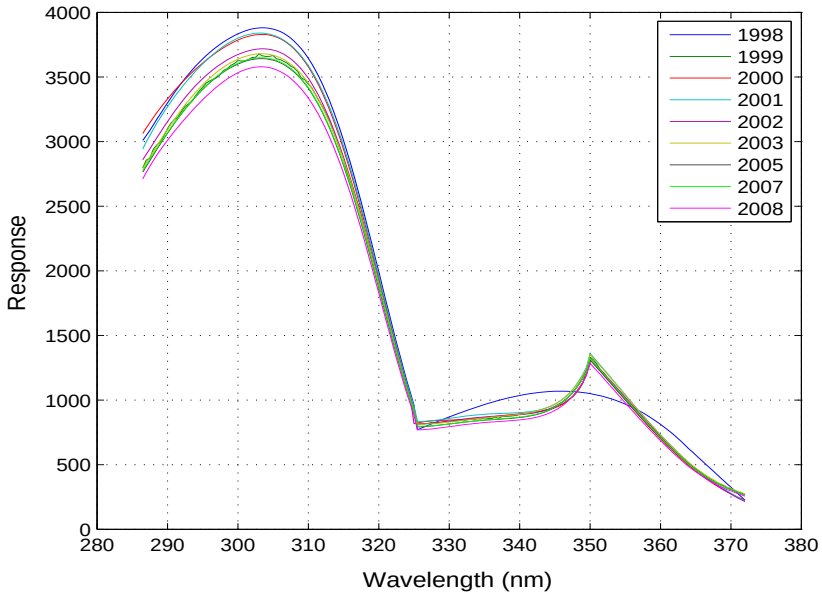

Figure 5.1: Brewer #042 response files measured from 1998 to 2008, by International Ozone Services Inc. [17].

the response files did not contain response data up to 372 nm, but rather to 363.5 nm or 370.5 nm, meaning that data measured at wavelengths between 363.5 or 370.5 nm and 372 nm had to be neglected if one wanted to use the corresponding response files for those years.

Ken Lamb at International Ozone Services Inc. [17] was consulted regarding this matter, and a new set of response files were later provided, all of which covered the 286.5 to 372 nm wavelength range. These may be seen in Figure 5.1. The unusual increase and then decrease in sensitivity at 350 nm was discovered after the UV calibration in 1998, which explains why the 1998 response file is of a dissimilar shape for the larger wavelengths. The other response files appear to be well correlated. According to the calibration reports, the reason why the response files for 2004 and 2006 are missing, is that the results compared well with the calibration of the previous years, and therefore no change to the response files was considered necessary. This means that for the years 2004 and 2006, the response files for the years 2003 and 2005, respectively, have been used.

It may be interesting to examine the effects of using "wrong" response files for the processing of Brewer data, in order to better understand the importance (or lack thereof) of performing the calibration procedures every year. Taking a closer look at Figure 5.1,

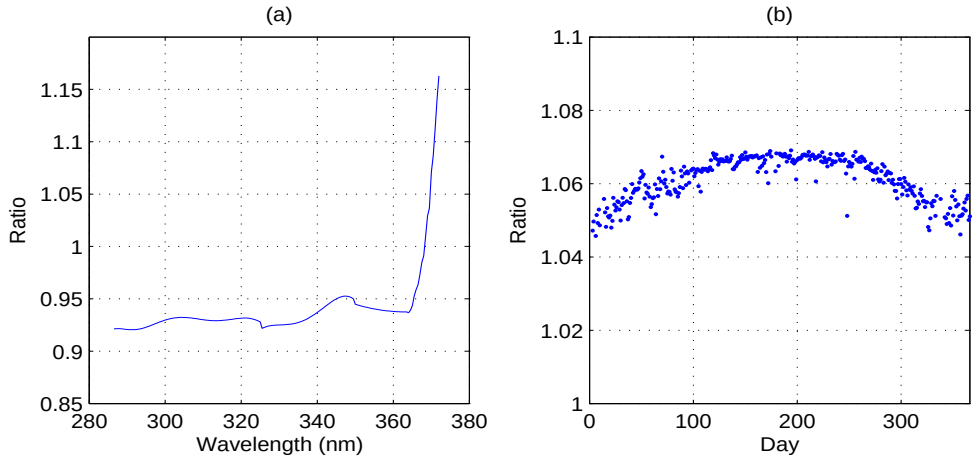

Figure 5.2: Comparison of the 2001 and 2008 response files. (a) is showing the ratio of the 2008 response file to the 2001 response file, whereas (b) is showing the ratio of the UV Indices obtained with Brewer data measured in 2008 and processed with the 2008 response file, to the same data processed with the 2001 response file.

and neglecting the odd shape of the 1998 response file, the greatest deviation found amongst the response files seems to be between the 2001 and 2008 files. Figure 5.2a shows the ratio of the 2008 response file to the 2001 response file. From 286.5 to ca. 365 nm, the 2008 response is about 5-8% lower than the 2001 response, whereas there is an abrupt change in ratio from ca. 0.94 to 1.16 for the wavelengths above ca. 365 nm, meaning that the 2008 response file has a higher response for the largest wavelengths. For the purpose of UV Index studies, however, this change in response for the largest wavelengths will probably not be noticeable, as the irradiances are weighted with the CIE action spectrum (described in Section 2.2.2), which is small for the upper part of the spectrum. Figure 5.2b shows the ratio of the UV Indices obtained with data processed with the 2008 response file, to the same data processed with the 2001 response file. The Brewer data used in this comparison is from the year 2008. The figure shows that the use of the 2008 response file results in UV Indices which are ca. 5-7% higher than the ones obtained using the 2001 response file.

It seems reasonable to assume that the 2008 to the 2001 ratio will be the largest deviation one may encounter when using "wrong" response files to obtain the UV Index (out of the final set of files provided from International Ozone Services Inc.). This suggests that the instrument has been relatively stable over the last decade, and that the use of a "wrong" reponse file should not play a significant role in the determination of the UV Index.

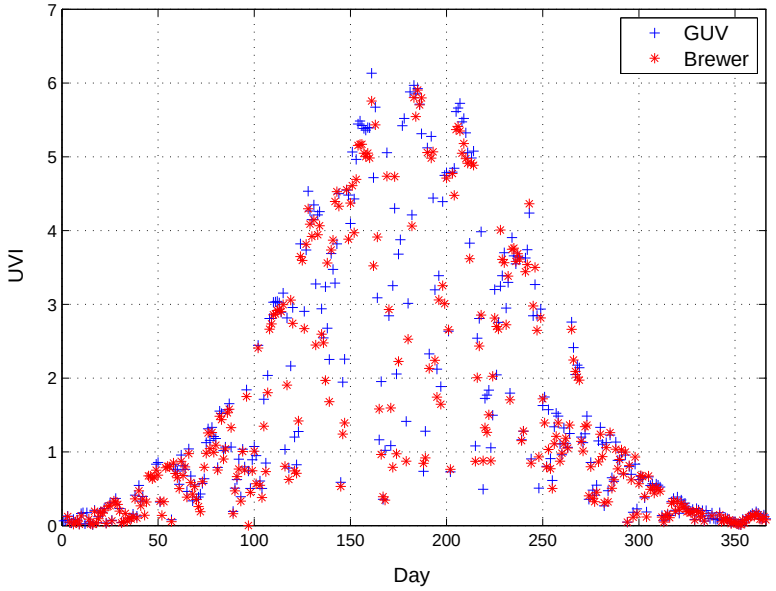

Figure 5.3: GUV-511 and Brewer #042 daily UV Index measured at noon throughout 2008.

The response files that have been stored in the Brewer computer and used for the daily generation of the DUV-files, belonged to the old set of response files provided from International Ozone Services Inc. The old versions of the response files deviated by less than 10% for the large part, however, a few of the wavelengths in the 2003 file were found to deviate by as much 45%. Hence, the UV Indices calculated from the data found in the DUV-files are generally not used for purposes of comparison in this thesis, which could have otherwise been interesting as a way to confirm the results obtained with the method presented in Section 4.3.

5.2 Measured UV Index, 2008

The UV Indices measured at noon with Brewer #042 and GUV-511 at Blindern throughout 2008 may be seen in Figure 5.3. The blue markers represent the GUV measurements and the red markers represent the Brewer measurements.

Figure 5.3 clearly shows how the UV Index reaches its peak around midsummer, which agrees well with the theory that a lower solar zenith angle increases the UV Index, since the sun is higher in the sky in the summer in Oslo. It was mentioned in Section 2.2.4 that a cloud cover greatly reduces the UVI. Oslo is not blessed with blue skies all

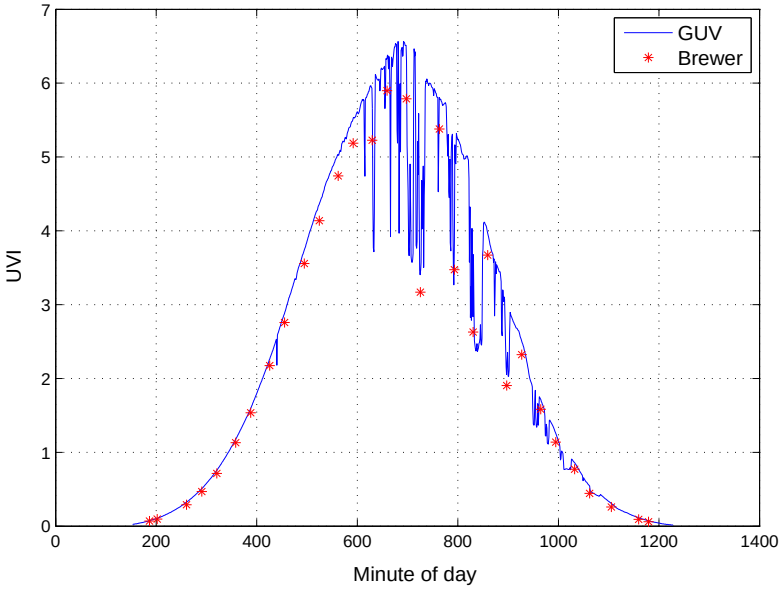

Figure 5.4: Complete set of Brewer #042 and GUV-511 UV Index measurements at Blindern on day 185 in 2008.

year round, and as the ground measurements are undertaken during all sorts of weather conditions, a considerable amount of the measurements are found below the seasonal maximum values.

The maximum UVI measured with GUV-511 in 2008 is just above 6, whereas the maximum Brewer #042 measurement is just below 6. According to Table 2.1, this is considered a "high level", but no higher than what one may expect in Oslo around midsummer. During the winter months, the measured and calculated UVI never exceeds 1, which is also in agreement with what one may expect, and is mainly due to the large midwinter solar zenith angles at Oslo's latitude (approximately 80^o to 85^o).

The maximum GUV measurement of the UVI is 6.13 and occurs on day 161. The maximum Brewer measurement is 5.91 and occurs on day 185. The reason why the UVI measurements do not necessarily cohere, is partially explained by the fact that these Brewer measurements are based on irradiances measured during the one scan found to be closest to noon, whereas the GUV measurements are based on the CIE-weighted UV dose rate averaged over an hour at noon. Figure 5.4 shows all GUV and Brewer measurements undertaken during one whole day in 2008. The blue line represents the UVI measured every minute with GUV, and the red markers represent Brewer measurements. As already explained in Section 2.2.4, the smooth curve during the first part

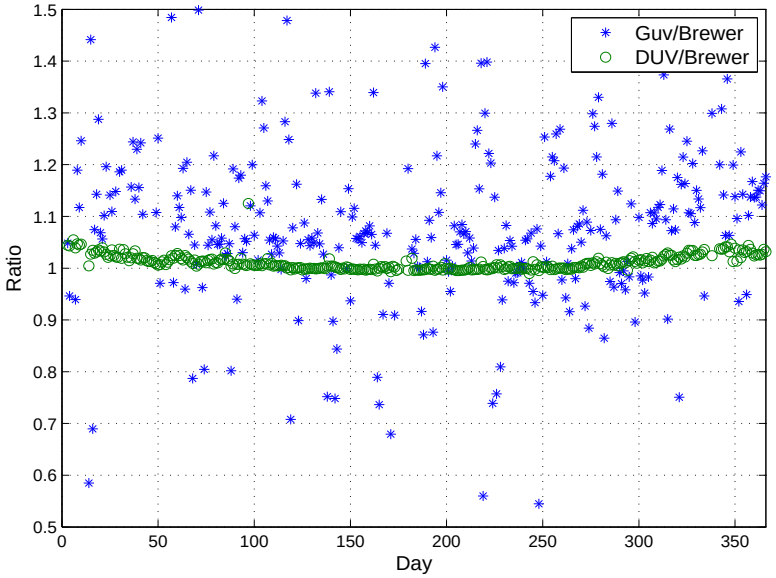

Figure 5.5: Daily GUV/Brewer UV Index ratios and DUV/Brewer UV Index ratios, measured at noon throughout 2008.

of the day, followed by dips from approximately one hour before noon throughout the late afternoon, indicate that the day started with stable, clear sky conditions, which was followed by scattered clouds for a large part of the day. The figure illustrates that the measurements undertaken during clear sky conditions cohere relatively well, which suggests that a single Brewer scan may well be compared to a one hour average for the GUV measurements during such weather conditions. However, the figure is also evidence that Brewer scans measured during non-stable conditions (which are plentiful throughout the year in Norway), may not necessarily be representative of the one hour average value obtained with the GUV instrument.

In Figure 5.5, the daily GUV/Brewer UV Index ratio measured at noon, throughout 2008, is shown in blue. Again, the Brewer measurements are based on irradiances measured during the one scan found to be closest to noon, whereas the GUV measurements are based on the CIE-weighted UV dose rate averaged over an hour at noon. The figure clearly shows that the comparison of UV Indices obtained with a single Brewer-scan and a one hour average for the GUV measurements, results in scattered ratios, making it rather hard to detect an apparent trend. Hence, one should perhaps look at other ways to compare these data. An attempt of this is conducted in the next three sections, during which monthly averages of the daily noon ratios will be presented first, followed

by a study of days with relatively stable weather conditions, which compares Brewer observations to GUV measurements obtained at the exact same minute as the Brewer scans (rather than GUV measurements averaged over an hour at noon).

The UV Indices obtained from Brewer's automatically generated DUV files (described in Section 3.1.7) in 2008, are also shown in Figure 5.5. In 2007 and 2008, the proper response files have been stored in the Brewer computer, which means that for the year 2008, the UV Indices obtained from the DUV files compare well to the UV Indices calculated from the raw data files. This is not generally the case, however, as the UV Indices obtained from the DUV files for other years were found to deviate by as much as 10-15%. The 1-3% deviation observed for the months at the beginning and end of the year in Figure 5.5, is caused by the use of a constant value for the upper part of the spectrum in the DUV calculations, as opposed to the method described in Section 4.2, which calculates the upper part of the spectrum according to seasonal variations.

5.3 Time Series 1998-2008

The monthly average GUV/Brewer UV Index ratios, from May 1998 to December 2008, are presented in Figures 5.6, 5.7 and 5.8. Figure 5.4 suggested that there seems to be a tendency of the GUV measurements being a bit higher than the Brewer measurements,

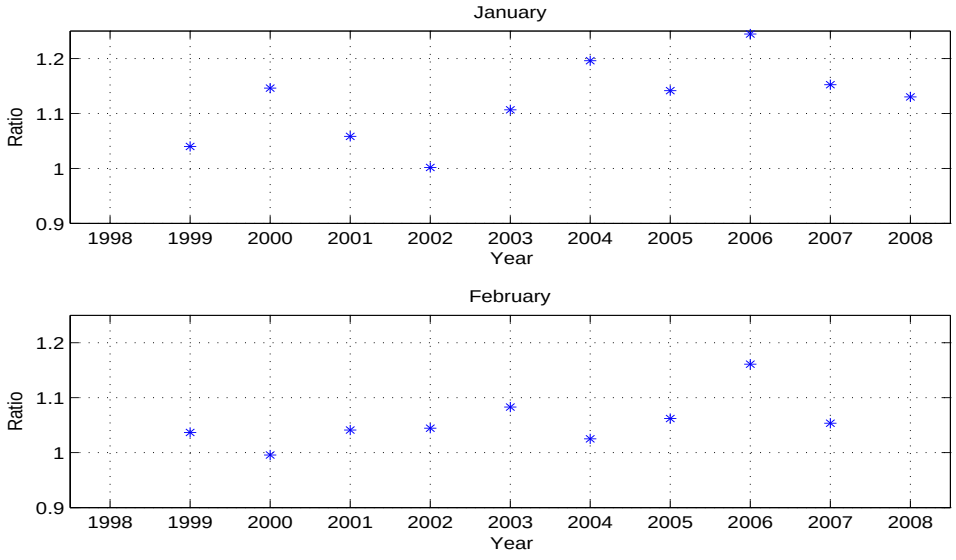

Figure 5.6: Monthly average Guv/Brewer UVI ratios January and February 1998-2008.

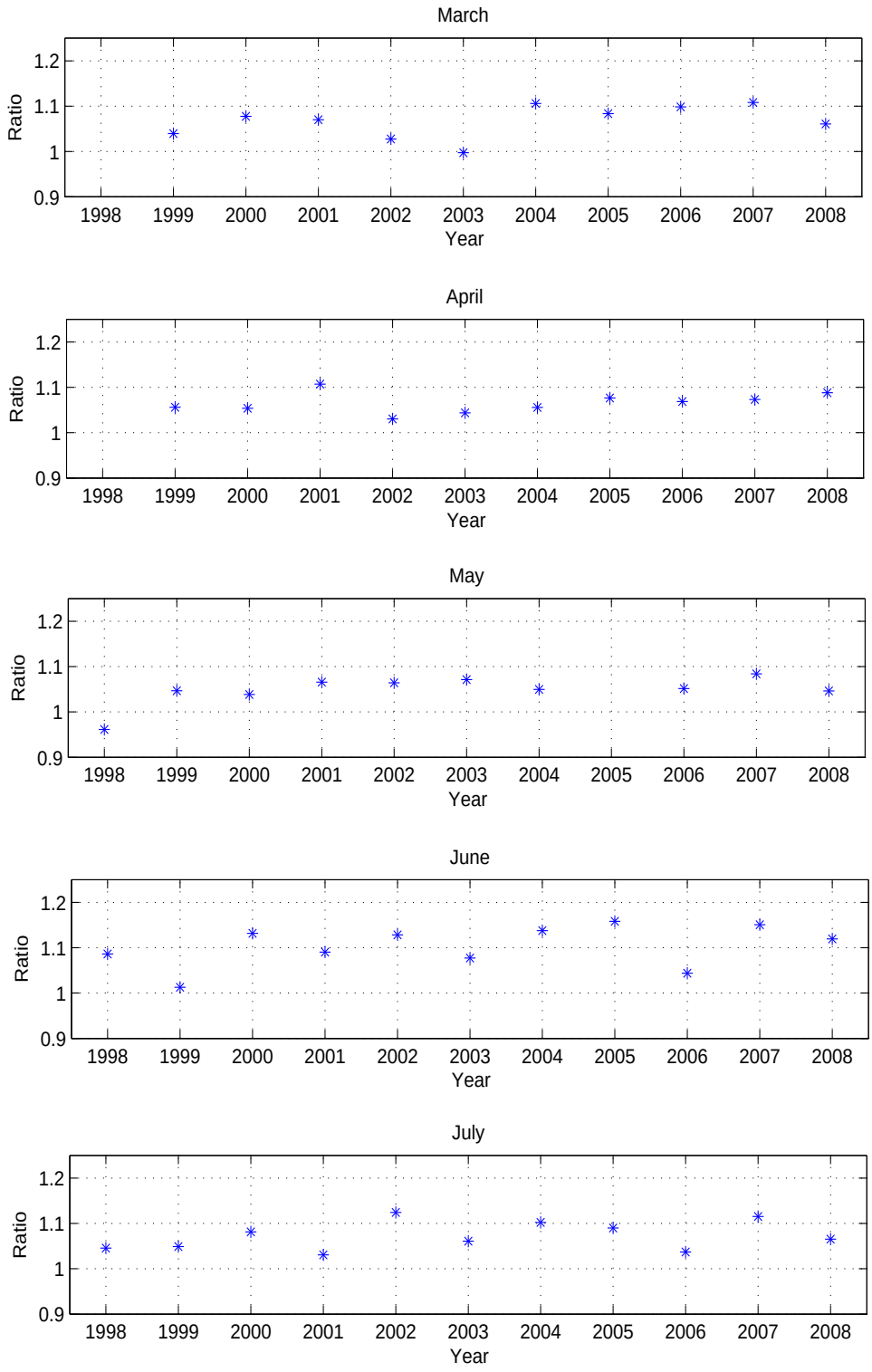

Figure 5.7: Monthly average Guv/Brewer UVI ratios March to July 1998-2008.

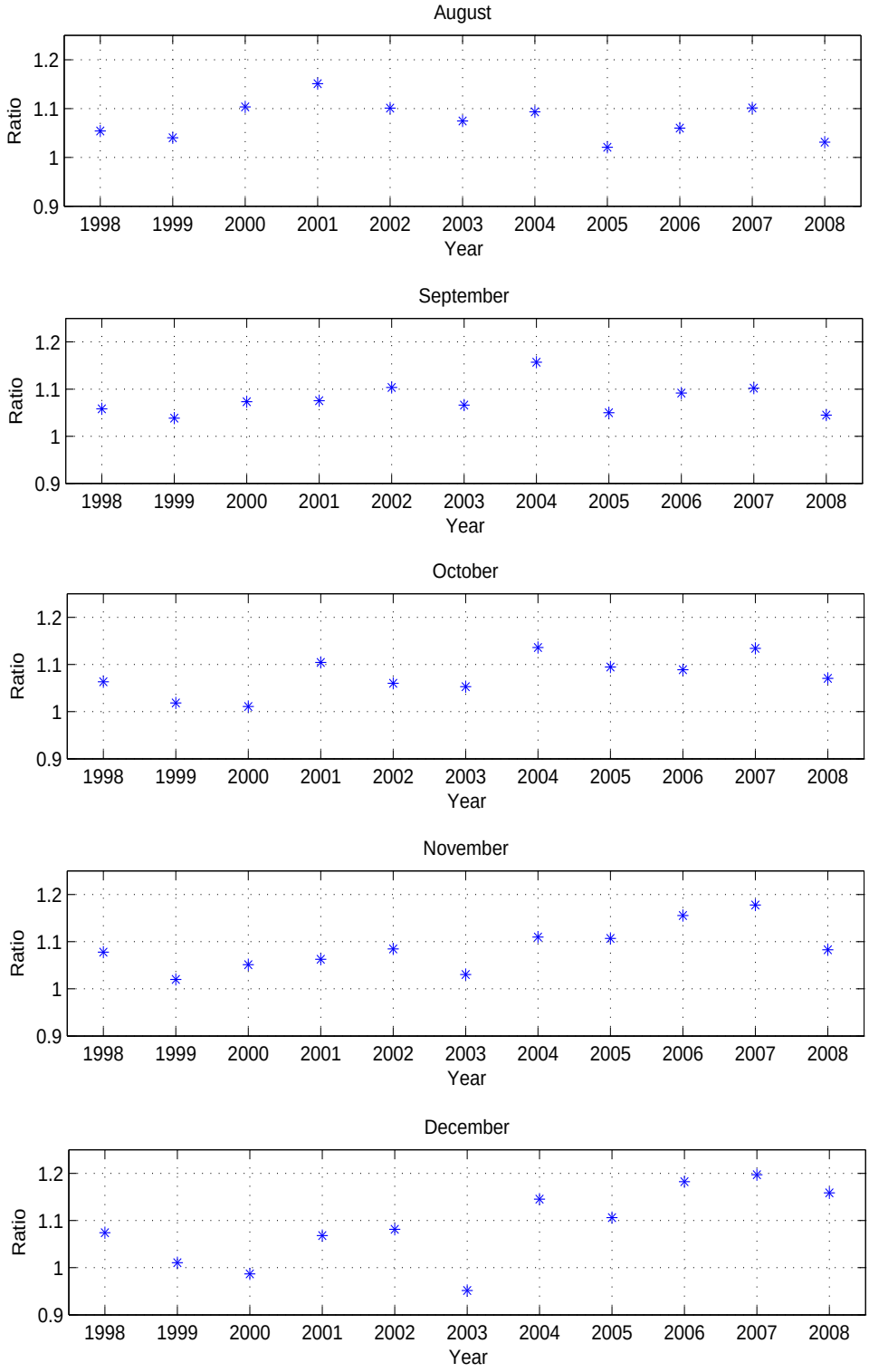

Figure 5.8: Monthly average Guv/Brewer UVI ratios August to December 1998-2008.

and the time series plots in Figures 5.6, 5.7 and 5.8 confirm this expectation to a great extent. This suggests that it may be easier to study monthly ratios, rather than daily ratios, when looking at a time series comparison of Brewer #042 and GUV-511 UV Index measurements.

From Figures 5.6, 5.7 and 5.8, the ratio is found to be between 1 and 1.15, for the months March-October (apart from for May 1998, which is when the new Brewer #042 measurements first started), suggesting that GUV measurements are from 0 to 15% higher than the Brewer measurements. The results for the darkest winter months deviate more, however, as mentioned before, the large midwinter solar zenith angles at Oslo's latitude cause a higher degree of uncertainty for these measurements, and they are therefore considered out of scope.

The Brewer #042 and GUV-511 instruments are normally calibrated in June, meaning that July measurements with both instruments may generally be considered as the most credible. Taking a closer look at the July ratios, one finds that the GUV-511 measurements are on average ca. 7% higher than the Brewer #042 measurements.

5.4 Comparison of Clear Sky Measurements

For this part of the study, the UV Indices measured at noon were compared to UV Indices calculated with `uvspec`, for the set of clear sky days selected in Section 4.6. A few of the input parameters tested in [10] were applied to these `uvspec` calculations. These include the 'Midlatitude Summer' `atmosphere_file` (which is the default for Blindern's latitude and longitude), the rural type aerosols for the lower 2 km of the atmosphere (assumed to be appropriate for Blindern as discussed in [10]), as well as a triangular `slit_function_file`, which resembles the distribution of the measurements over the slit width of the instrument, to be convolved with the calculated spectrum in order to make the calculated results better resemble the measured results.

Figure 5.9a shows the measured and calculated absolute values, which indicate a relatively good agreement between the GUV-511, Brewer #042 and `uvspec` UV Indices. Figure 5.9b shows the ratios of the `uvspec`/Brewer and GUV/Brewer UV Indices, which support the above suggestion that GUV-511 measurements are approximately 7% higher than Brewer #042 measurements, at least for stable clear sky measurements. The coherence between the `uvspec` and Brewer UV Indices is more varied. This may be due to a number of reasons, such as the use of `uvspec` atmosphere and aerosol files which

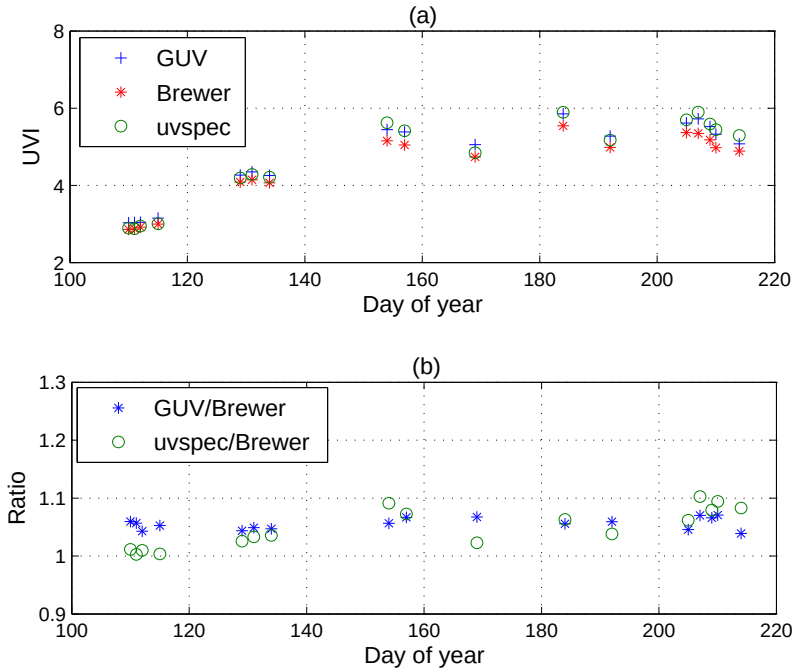

Figure 5.9: (a) shows GUV, Brewer and uvspec UV Indices for clear sky days in 2008. (b) shows the UV Index ratios uvspec/Brewer and GUV/Brewer for clear sky days in 2008.

do not match the actual atmospheric conditions on the given set of days. Another possible explanation for the relatively low ratio found for the first four days, all of which occur in April, may be that snow in the areas surrounding Blindern causes a higher ground albedo, and thus contributes to the total measured UV Index. Snow depth data available at [15] show that there were substantial amounts of snow in Nordmarka (a forested area North of Blindern) throughout April 2008, giving supporting evidence to this explanation.

5.5 Comparison of Measurements on Overcast Days

In this section, UV Indices measured on days with a relatively stable overcast weather situation were compared. As `uvspec` calculations of UV irradiances on cloudy days are vastly more complicated than on clear sky days, and therefore considered out of scope, only GUV and Brewer data are presented in this section.

Figure 5.10a shows the measured absolute values, whereas Figure 5.10b shows the ratio GUV/Brewer. The plots indicate a relatively good agreement between the GUV-511

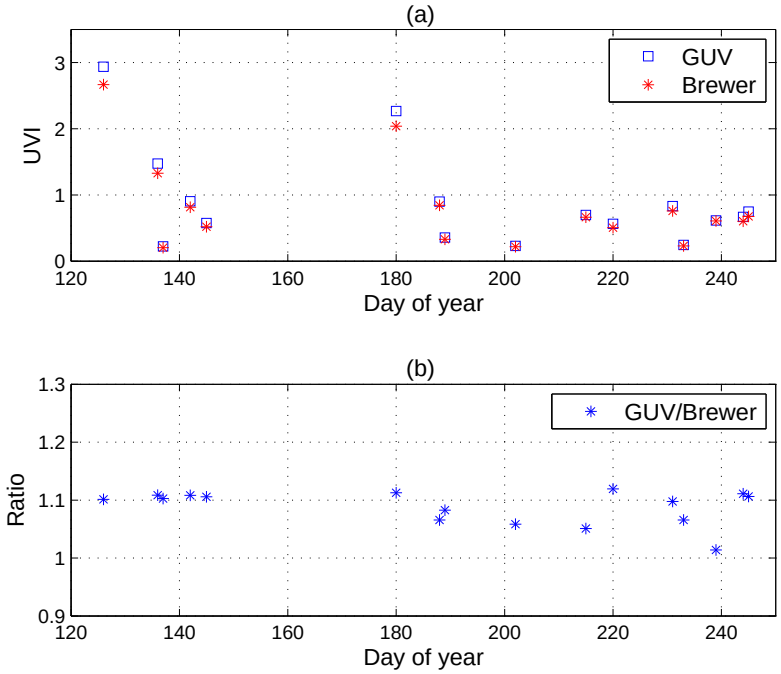

Figure 5.10: (a) shows UV Index measurements for GUV and Brewer on overcast days in 2008. (b) shows the UV Index ratio GUV/Brewer measured on overcast days in 2008.

and Brewer #042 UV Indices, suggesting that the two instruments provide relatively similar results also for overcast weather situations.

The average ratio obtained for the overcast days seems closer to 1.1 than the 1.07 value which was indicated as a possible average GUV/Brewer ratio in the previous sections. However, the degree of uncertainty is much higher for these measurements than the clear sky measurements, due to the facts that the absolute values of the UV Indices studied here are very low (all but three of the measurements are below a UV Index of 1), and that somewhat stable overcast conditions are very difficult to obtain. All in all, it is difficult to conclude anything about whether the GUV/Brewer ratio is actually higher on overcast days, and this would require a much more thorough study to be conducted.

5.6 Single- vs. Double-Monochromator Measurements

In this section, complete spectra obtained from Brewer #042, the Bentham DM 150 Spectroradiometer at Østerås and clear sky `uvspec` calculations, for day 209 in 2008, are compared. On this day, the cloud transmission measured by the GUV-511 instrument

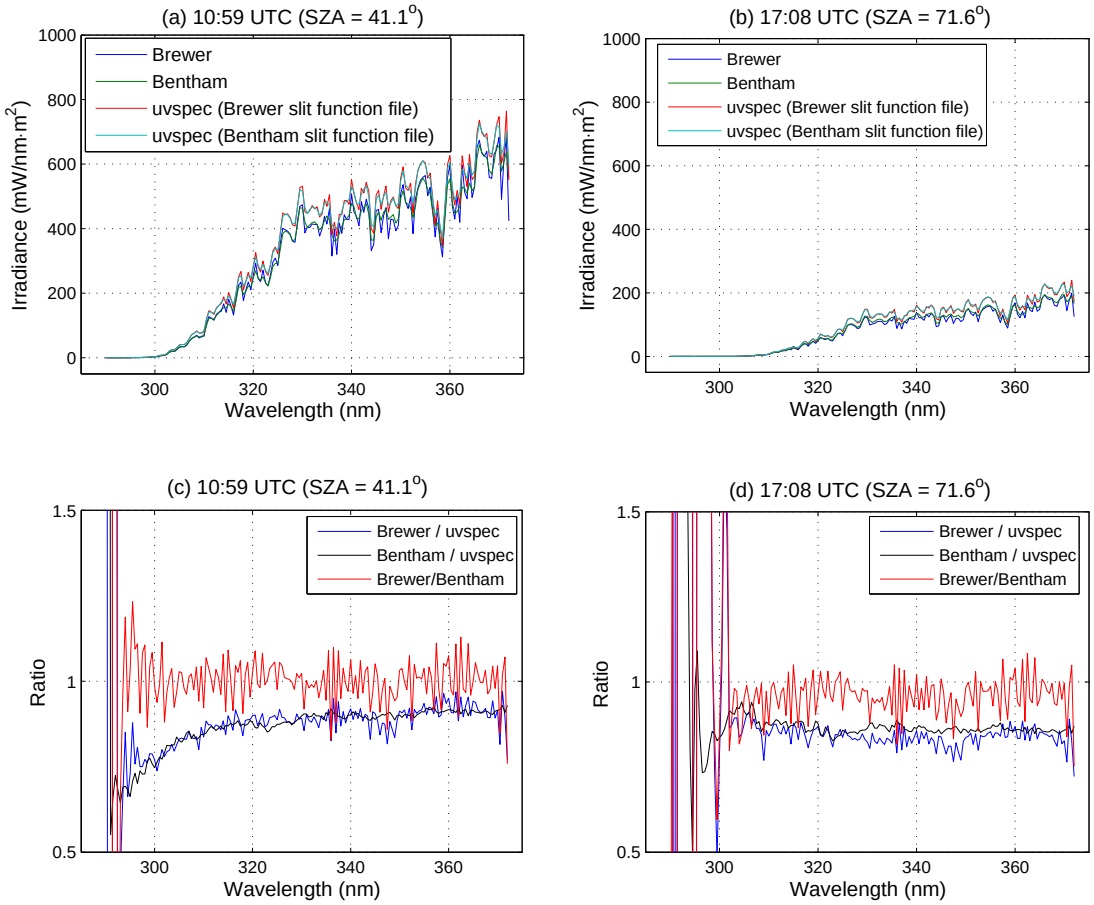

Figure 5.11: (a) and (b) show complete Brewer, Bentham and uvspec spectra at noon (10:59 UTC) and in the evening (17:08 UTC), respectively, for day 209 in 2008. (c) and (d) show ratios of the same spectra at noon (10:59 UTC) and in the evening (17:08 UTC), respectively. The solar zenith angle (SZA), as indicated in the figures, was 41.1^o for the noon measurements and 71.6^o for the evening measurements.

was above 95% throughout the entire day, indicating blue sky conditions from early morning until late evening.

The ozone input to `uvspec` has been obtained from Brewer measurements, as these are considered to be quality assured [2]. A triangular `slit_function_file`, which resembles the distribution of the measurements over the slit width of the instrument (see Section 3.4.3), has been used in the `uvspec` calculations. This requires the input of the FWHM (full width at half maximum) of the instruments, which is 0.6 nm for Brewer and 0.87 nm for Bentham. As the FWHM is different for the two instruments, one obtains one set of model spectra supposed to resemble the Brewer instrument and one set of model spectra supposed to resemble the Bentham instrument.

The measured and calculated spectra at noon (10:59 UTC) and in the early evening (17:08 UTC), are shown in Figures 5.11a and b, respectively. One may see from the figures that the calculated irradiances are higher than the measured irradiances, for most of the wavelengths in both scans. This may be due to the fact that aerosols are not applied in the simulations; this would reduce the calculated irradiance as described in [10]. The use of a more appropriate atmosphere file than the standard U.S. atmosphere file could also have resulted in slightly decreased irradiance values [10].

From Figures 5.11a and b, one sees that the irradiance is substantially reduced at all wavelengths in the evening, compared to the noon measurements, as one would expect. Specifically, one may see that hardly any irradiance below 310 nm reaches the ground during the evening scan, whereas irradiance as low as 300 nm is measured in the noon scan. This may be due to the fact that scattering and absorption increases for decreasing wavelengths in the UVA- and UVB-regions of the spectrum (due to ozone absorption and Rayleigh-scattering) [32], and the lower solar zenith angle in the evening means that the radiation has to pass through a longer path in the atmosphere, allowing for more scattering and absorption of smaller wavelengths, relative to that which the larger wavelengths experience. This also implies that the larger wavelenghts will contribute to a greater fraction of the evening UVI than they do to the noon UVI.

5.6.1 Stray Light Performance

According to [13], Environment Canada recommends the Mk III Brewer as significantly superior to the Mk II and Mk IV (hence, Brewer #042) for measurements of solar radiation and ozone in the UV region of the spectrum. This is because the double-monochromator optical system used in the Mk III has a much improved stray light performance, compared to the single-monochromator of the Mk II and Mk IV. Campaigns in Finland have also shown that double-monochromator ozone measurements, performed at large solar zenith angles during periods with high amounts of ozone in the atmosphere, are considerably improved compared to single-monochromator measurements [6].

Figures 5.11c and d show the ratios Brewer/Bentham and measured/calculated spectra for the noon and evening scans, respectively. The 'noise' which may be seen for the Brewer/Bentham ratio is due to the different slit functions of the two instruments, and is a common effect observed when two different spectroradiometers are compared. Usually, one may compensate for this effect to obtain more smooth curves. As discussed in [10], the measurement/model ratios would also fluctuate in a similar manner, if the slit functions of the instruments had not been considered in the model calculations.

Table 5.1: UV Indices obtained from every Brewer scan from noon throughout the evening of day 209 in 2008. Also shown are the UV Indices obtained from simultaneous Bentham scans, as well as the ratio Brewer/Bentham, and the solar zenith angle (SZA) at the time of the measurements.

SZA [^{o}]	**Brewer** [UVI]	**Bentham** [UVI]	**Brewer/Bentham** [$RATIO$]
41.1	5.1717	5.1634	1.0016
40.9	5.2167	5.2179	0.9998
41.6	5.0654	5.0848	0.9962
43.0	4.7812	4.7622	1.0040
45.5	4.2751	4.2595	1.0037
48.1	3.7516	3.7226	1.0078
52.0	3.0811	3.0036	1.0258
55.4	2.5362	2.4626	1.0299
59.4	1.8695	1.9414	0.9630
64.0	1.4023	1.3255	1.0579
67.8	0.9036	0.9437	0.9575
71.6	0.6098	0.6359	0.9591
77.8	0.2705	0.2962	0.9129

From the figures, one sees that for the noon scan, both the Brewer and the Bentham measurements seem reasonably well correlated with each other as well as with their respective `uvspec` spectra, even for a few wavelengths below 300 nm. For the evening scan, one sees more fluctuations for the lower wavelengths, which is probably due to stray light and dark current in the instrument [20]. However, if the purpose of the measurements is UV Index studies, and not ozone measurements, one may assume that a high precision for the shortest wavelengths is generally not crucial for measurements at large solar zenith angles, as the above discussion showed that the larger wavelenghts will contribute to a greater fraction of the evening UVI than they do to the noon UVI.

It may be interesting to compare the measured Brewer and Bentham UV Indices for various solar zenith angles, to see whether a deviation between the two occurs at a certain solar zenith angle. Table 5.1 shows the UV Indices calculated for every Brewer scan from noon throughout the evening of day 209 in 2008, together with the solar zenith angle (SZA). UV Indices obtained from simultaneous Bentham scans are also shown, as well as the ratio Brewer/Bentham. The data provided in the table suggest that the Brewer and Bentham measurements correlate very well for the smallest solar zenith angles, with less than 1% deviation for solar zenith angles up to 48.1^o. However, even for solar zenith angles up to 71.6^o, where the total UVI is well below 1, the results are within 5-6%, suggesting that single-monochromator instruments may well be used for UV Index measurements, even at relatively large solar zenith angles.

Chapter 6

Conclusion

The purpose of this thesis was to study UV data recorded with the Brewer Mk V Spectrophotometer (#042) at Blindern in Oslo. The complete processing chain from raw signal to UV spectra was presented, together with a method used to obtain the UV Index from these measurements. This method involved the use of the radiative transfer model `uvspec` to estimate the upper part of the spectrum, as Brewer Mk V measures UV irradiances from 286.5 to 372 nm and one needs spectra from 290 to 400 nm to obtain the UV Index.

It was discovered that incorrect response files had been provided from the company responsible for the yearly calibration of the instrument. A revised set of response files was obtained (Figure 5.1), allowing for a discussion of the stability of the instrument. The examination of the instrument's response from 1998 to 2008 indicated that Brewer #042 has been relatively stable over the last decade. The greatest deviation in response files was found between the years 2001 and 2008, with a deviation in response of less than 8% for most wavelengths (Figure 5.2).

The Brewer UV Index observations were compared to UV Index measurements obtained with a moderate bandwidth GUV-511 instrument. A 1998 to 2008 time series of the monthly average GUV/Brewer ratio was presented (Figures 5.6, 5.7 and 5.8), as well as a more detailed study of the UV Index measured on clear sky days (Figure 5.9). These results indicated that the GUV measurements on average were ca. 7% higher than the Brewer measurements.

A study of the UV Index measured on overcast days in 2008 was also conducted. As expected, these results deviated more than the results obtained for the clear sky days

(Figure 5.10), probably due to the non-stable atmospheric conditions induced by clouds during measurements. The results suggested a slightly higher average deviation than the above-mentioned 7%, however, a much more thorough study would be necessary before one could expand on this.

Finally, Brewer #042, being equipped with a single-monochromator, was compared to the Bentham DM 150 Spectroradiometer at Østerås, which is equipped with a double-monochromator. A comparison of spectral UV showed a reasonably good correlation for measurements undertaken at a solar zenith angle of ca. 41.1^o, even for wavelengths shorter than 300 nm. With a solar zenith angle of 71.6^o, however, the Brewer measurements around 300 nm deviated substantially from the Bentham observations, indicating a poorer stray light performance for the Brewer instrument (Figure 5.11d).

The UV Indices obtained with the Bentham and Brewer instruments for various solar zenith angles were also compared. These were found to deviate by less than 6% for solar zenith angles up to 71.6^o (Table 5.1). Hence, if the purpose of the measurements is UV Index studies, one may assume that a high precision for the shortest wavelengths is generally not crucial for measurements at large solar zenith angles.

The results obtained in this thesis indicate that Brewer #042 has been a relatively stable instrument over the last decade. A good correlation between GUV-511 observations and Brewer measurements is also seen, with an average deviation of approximately 7%. This may be considered as very reasonable, as it is difficult to measure spectral global irradiance in the UV within an uncertainty of ca. 5%, even for the best instruments available today [2].

6.1 Future Work

As mentioned in Section 2.4, the difficulty of measuring the spectral UV within an uncertainty of ca. 5% has to do with the sources of error and uncertainties associated with measurements of spectral global irradiance in the UV. These include the cosine response and temperature dependence of the instrument, wavelength misalignment, spectral resolution and timing errors, stray light, noise, and the stability and calibration of the instrument.

Quality assurance of data recorded with the Brewer instrument may include daily maintenance, laboratory characterizations, calculation of long-term spectral responsivity, data processing and quality assessment. Very few of these are being performed for Brewer

#042, meaning that there is great potential for the improvement of the uncertainty of the measurements. A continued study of these measurements should therefore consider looking more into the quality assurance of the measurements, in order to obtain high quality spectra.

It should be mentioned that although the determination of certain sources of error may be improved by frequent laboratory characterizations, one should at the same time be careful with moving the instrument around too much, as movement of the instrument may in itself cause alterations to the stability of the instrument [2]. The stability observed for Brewer #042 in this thesis may well be due to the fact that this instrument has rarely been moved over the last decade.

Brewer #042 has been in operation since 1990, however, as mentioned in Section 1.2, these data have not been studied up until now. The instrument went through several major modifications up until 1998, and the data obtained from the first 8 years of operation are stored in a variety of different formats and folder structures, making it quite the job to sort them all out. If this task were to be carried out, one would obtain one of the longest spectral UV time series in Europe, which could allow for a study of UV radiation level trends. A trend analysis may for instance be interesting as part of a climate change study.

A study of the data obtained in Brewer #042's early years of operations would also open for an opportunity to study possible long-range effects of the volcanic eruption of Mount Pinatubo in 1991. This major eruption injected large amounts of aerosols into the stratosphere, and the aerosols formed a global layer of sulfuric acid haze over the following months. Several studies undertaken with Brewer spectrophotometers located at different continents, such as [27] and [8], have discussed the effects caused by the Mount Pinatubo eruption, and it could be very interesting to investigate to what extent the observations at Blindern were influenced.

Bibliography

[1] G.P. Anderson, S.A. Clough, F.X. Kneizys, J.H. Chetwynd, and E.P. Shettle. AFGL atmospheric constituent profiles (0-120 km). AFGL-TR-86-0110, Air Force Geophysics Laboratory, Hanscom Air Force Base, MA, USA, 1986.

[2] A. Dahlback. Department of Physics, University of Oslo. Personal interviews, February 2008 - March 2009.

[3] A. Dahlback. Measurements of biologically effective UV doses, total ozone abundances, and cloud effects with multichannel, moderate bandwidth filter instruments. *Applied Optics*, 35(33):6514–6521, 1996.

[4] A. Dahlback and K. Stamnes. A new spherical model for computing the radiation field available for photolysis and heating at twilight. *Planetary and Space Science*, 39:671–683, 1991.

[5] How does the Dobson Spectrophotometer Work? Stratospheric Ozone Research in Fairbanks Alaska. [Available online (visited 6. March 2009) `http://ozone.gi.alaska.edu/dobson.htm`].

[6] SAUNA. Sodankylä Total Column Ozone Intercomparison. 20. March - 14. April, 2006. Arctic Research Centre of the Finnish Meteorological Institute. [Available online (visited 9. March 2009) `http://fmiarc.fmi.fi/SAUNA/`].

[7] Earth System Research Laboratory Global Monitoring Division. Brewer MkIV spectrophotometer. [Available online (visited 6. March 2009) `http://www.esrl.noaa.gov/gmd/grad/neubrew/MkIV.jsp`].

[8] J. Gröbner and C. Meleti. Aerosol optical depth in the UVB and visible wavelength range from Brewer spectrophotometer direct irradiance measurements: 1991–2002. *Journal of Geophysical Research*, 109, 2004.

[9] Biospherical Instruments Inc., 5340 Riley Street, San Diego, CA 92110, USA. [Available online (visited 6. March 2009) http://www.biospherical.com/].

[10] Kristin Karthum Hansen. *Project Work Physics. A study of UVSPEC calculations and ground measurements of the UV Index in Oslo.* Department of Physics, Norwegian University of Science and Technology, 2008.

[11] E. Hecht. *Optics.* Addison Wesley, Fourth International edition, 2002.

[12] T. Henriksen, E.K. Henriksen, and T. Svendby. *Temahefte 1, Vår strålende verden: Deilig er den himmel blå.* Department of Physics, University of Oslo, 2005.

[13] Kipp & Zonen Inc. Brewer Spectrophotometer. [Available online (visited 6. March 2009) http://www.kippzonen.com/?product/5051/Brewer+MKIII.aspx].

[14] SCI-TEC Instruments Inc. BREWER MKIV Spectrophotometer Operator's Manual, August 1999. [Available online (visited 6. March 2009) http://www.kippzonen.com/?downloadcategory/39212/Discontinued+Brewers].

[15] Norwegian Meteorological Institute, Norwegian Mapping Authority, and Norwegian Water Resources and Energy Directorate. senorge.no - snow, weather, water and climate in norway. [Available online (visited 6. March 2009) http://www.senorge.no/].

[16] Royal Netherlands Meteorological Institute. OMI total ozone. [Available online (visited 24. February 2009) http://www.knmi.nl/omi/publ-nl/metingen/ozone/metingen_o3_nrt.html].

[17] International Ozone Services Inc., 43 Lehar Cres., Toronto Ontario, Canada M2H1J4. [Available online (visited 6. March 2009) http://www.io3.ca/].

[18] T. Koskela. Temperature Characterisation of the UV response. Poster presented at the 8th Biennial WMO/GAW Brewer Users Group Meeting, INTA, El Arenosillo, SPAIN, 2003.

[19] K. Lakkala, A. Arola, A. Heikkilä, J. Kaurola, T. Koskela, E. Kyrö, A. Lindfors, O. Meinander, A. Tanskanen, J. Gröbner, and G. Hülsen. Quality assurance of the brewer spectral uv measurements in finland. *Atmospheric Chemistry and Physics*, 8:3369–3383, 2008.

[20] Bentham Instruments Ltd. A guide to spectroradiometry, instruments and applications for the ultraviolet, Issue 2.00, January 1997. [Available online (visited 6. March 2009) `http://www.bentham.co.uk/pdf/UVGuide.pdf`].

[21] B. Mayer. Radiative transfer modelling. [Available online (visited 6. March 2009) `http://www.bmayer.de/index.html?uvspec.html\&1`].

[22] B. Mayer and A. Kylling. Technical note: The libradtran software package for radiative transfer calculations - description and examples of use. *Atmospheric Chemistry and Physics*, 5:1855–1877, 2005.

[23] B. Mayer, A. Kylling, U. Hamann, and C. Emde. libradtran, library for radiative transfer calculations, edition 1.0 for libRadtran version 1.4, December 2008. [Available online (visited 6. March 2009) `http://www.libradtran.org/`].

[24] A.F. McKinlay and B.L. Diffey. A reference action spectrum for ultra-violet induced erythema in human skin. *J. Commission Internationale de l'Eclairage*, 6:17–22, 1987.

[25] Lars Opedal. *Hovedoppgave i fysikk. UV-målinger med Brewer MKIV Ozone Spectrophotometer: Kalibrering og kvalitativ vurdering av målingene.* Department of Physics, University of Oslo, 1996.

[26] World Health Organization. Global solar UV index, a practical guide, fact sheet 271, Geneva, Switzerland, 2002. [Available online (visited 6. March 2009) `http://www.who.int/mediacentre/factsheets/fs271/en/`].

[27] Y. Sahai, V. W. J. H. Kirchhoff, and P. C. Alvalá. Pinatubo eruptions: effects on stratospheric O3 and SO2 over Brasil. *Journal of Atmospheric and Solar-Terrestrial Physics*, 59(3):265–269, 1997.

[28] M.L. Salby. *Fundamentals of Atmospheric Physics.* Academic Press, 1996.

[29] G. Seckmeyer and G. Bernhard. Cosine error correction of spectral UV-irradiances. *Proceedings of Spie, Atmospheric Radiation, K. H. Stamnes; Ed.*, 2049:140–151, 1993.

[30] E.P. Shettle. Models of aerosols, clouds and precipitation for atmospheric propagation studies. In *AGARD Conference Proceedings No. 454, Atmospheric propagation in the UV, visible, IR and mm-wave region and related system aspects*, 1989.

[31] K. Stamnes, S.C. Tsay, W. Wiscombe, and K. Jayaweera. A numerically stable algorithm for discrete-ordinate-method radiative transfer in multiple scattering and emitting layered media. *Applied Optics*, 27:2502–2509, 1988.

[32] G.E. Thomas and K. Stamnes. *Radiative Transfer in the Atmosphere and Ocean.* Cambridge University Press, 1999.

[33] E. Weatherhead, D. Theisen, A. Stevermer, J. Enagonio, B. Rabinovitch, P. Disterhoft, K. Lantz, R. Meltzer, J. Sabburg, J. DeLuisi, J. Rives, and J. Shreffler. Temperature dependence of the brewer ultraviolet data. *Journal of Geophysical Research*, 106:34121–34129, 2001.

[34] Ozone and UV radiation monitoring. Department of Physics, University of Oslo. [Available online (visited 6. March 2009) `http://www.fys.uio.no/plasma/ozone/`].

[35] Toms news. NASA. Ozone Processing Team - NASA/GSFC Code 613.3. [Available online (visited 6. March 2009) `http://jwocky.gsfc.nasa.gov/news/news.html`].

[36] U.S. standard atmosphere 1976. NOAA (1976), NASA, U.S. Air Force, Gov. Print. Off., Washington, D.C. [Available online (visited 6. March 2009) `http://modelweb.gsfc.nasa.gov/atmos/us_standard.html`].

[37] UV-indeks. Norwegian Radiation Protection Authority (Statens Strålevern). [Available online (visited 6. March 2009) `http://www.nrpa.no/`].

[38] UV radiation monitoring: UV index and UV dose. Tropospheric Emission Monitoring Internet Service, KNMI. [Available online (visited 6. March 2009) `http://www.temis.nl/uvradiation/info/uvindex.html`].

[39] Ozone. United States Environmental Protection Agency. [Available online (visited 6. March 2009) `http://www.epa.gov/ozone/`].

[40] Image: Solar spectrum.png. Wikipedia Images. [Available online (visited 6. March 2009) `http://en.wikipedia.org/wiki/Image:Solar_Spectrum.png`].

Appendix A

Matlab Programming

The Matlab program seen in Appendix A.1 has been created and used as a part of this project work, and is described in Section 4.3.

A.1 brewerUVItimeSeries.m

```
clear all;
close all;

year = input('Input wanted year [YY] (between 90 and 08): ', 's');
dayStart = input('Input wanted start day [ddd], between 1 and 366: ');
dayEnd = input('Input wanted end day [ddd], between 1 and 366: ');
responseFile = input('Input response file name (e.g. UVR17702.042): ', 's');

uviFID = fopen( ['BrUVI_' year], 'wt' );
fprintf ( uviFID, '%s \t', 'Day' );
fprintf ( uviFID, '%s \n', 'UVI_br' );

% READ SELECTED RESPONSE FILE
[response, endWL] = readResponseFile(responseFile);

% FOR EACH DAY...
j=1;
for day=dayStart:1:dayEnd
    if (day < 10) dayNumber = ['00' int2str(day)];
    elseif (day < 100) dayNumber = ['0' int2str(day)];
    else dayNumber = int2str(day);
```

```
    end
    fprintf ( uviFID, '%s \t', dayNumber );
    try
        % TRY: READ DATA FILE FOR EACH DAY, PROCESS DATA, CALCULATE UVI
        noonRawScan = readDataFile(dayNumber, year);
        processedScan = processData(noonRawScan);
        [tailUVI, avg3u] = calcTailUVI(day, endWL);
        UVI = calcUVI(processedScan, response, endWL, tailUVI, avg3u);
        fprintf ( uviFID, '%3.4f \n', UVI );
    catch
        % CATCH: IF SOMETHING GOES WRONG WRITE 'Not a Number' TO FILE
        fprintf ( uviFID, '%s \n', 'NaN' );
    end
end
fclose ( uviFID );
```

****

```
function [response, endWL] = readResponseFile(responseFile)

% READ RESPONSE FILE
responseFID = fopen ( ['../../../data/br/respons/rfiler/' responseFile] );
l = 1;
wl_wanted = 2900;
while ( ~feof(responseFID) )
    responseData = textscan ( responseFID, '%f %f', 1 );
    response(l).wl = responseData{1};
    response(l).value = responseData{2};
    if ( response(l).wl == wl_wanted ) % Starting to read/store at 2900
        l = l+1;
        wl_wanted = wl_wanted + 5;
    end
end
fclose(responseFID);

endWL = (floor(response(l-1).wl/10))*10;
```

****

```
function [noonRawScan] = readDataFile(dayNumber, year)

% READ DATA FILE
rawDataFID = fopen(['../../../data/br/uvdata-konv/uv-' year '/' 'uv' dayNumber year '.042']);
if(rawDataFID == -1)
    rawDataFID = fopen(['../../../data/br/uvdata-konv/uv-' year '/' 'UV' dayNumber year '.042']);
end

i = 1;
while ( ~feof(rawDataFID) )
    headerArray = textscan(rawDataFID,'%*s %*s %*s %*s %*s %*s %*s %s %*s %*s %*s %*s %s',1);
    DT = headerArray{1};
    dark = headerArray{2};
    readLine = textscan ( rawDataFID, '%s %f %*f %f', 1 );
    if ( isempty(cell2mat(dark)) ) || ( strcmp(readLine{1},'end') )
         continue;
    end
    scan(i).dark = str2num(cell2mat(dark));
    scan(i).DT = str2num(cell2mat(DT));
    j = 1;
    wl_start = 2900;
    while ( strcmp(readLine{1},'end') ~= 1 )
        scan(i).line(j).time = str2num(cell2mat(readLine{1}));
        scan(i).line(j).wl = readLine{2};
        scan(i).line(j).raw = readLine{3};
        if (scan(i).line(j).wl == wl_start ) % Starting to read/store at 2900
            j = j+1;
            wl_start = wl_start + 5;
        end
        readLine = textscan ( rawDataFID, '%s %f %*f %f', 1 );
    end
    i = i+1;
end
fclose(rawDataFID);

% FIND SCAN WITH 325nm-MEASUREMENT CLOSEST TO NOON
noon = 0;
minDeviation = Inf; % infinity
for i=1:1:length(scan)
    for j=1:1:length(scan(i).line)
        if (scan(i).line(j).wl == 3250 )
            duv325 = j;
```

```
        end
    end
    if (i>2) && (abs(660-scan(i).line(duv325).time)<minDeviation) ...
       && (scan(i).line(duv325).time > scan(i-1).line(duv325).time )
        noon = i;
        minDeviation = abs(660 - scan(i).line(duv325).time);
    end
end

if ( minDeviation < 25 )
    noonRawScan = scan(noon);
else
    noonRawScan = NaN;
end
```

****

```
function [processedScan] = processData(noonScan)

% COMPENSATE FOR # CYCLES & USE INTERVAL-SCALING FACTOR (IT)
IT = 0.1147;
CY = 1;
for j=1:1:length(noonScan.line)
    % CALCULATE COUNT RATE N
    noonScan.line(j).N = ...
        ( ( noonScan.line(j).raw - noonScan.dark ) * 2 ) / ( CY * IT );
    % ITERATION: CORRECT FOR DEAD TIME (DT) TO FIND TRUE COUNT RATE
    noonScan.line(j).No = noonScan.line(j).N;
    for k=1:1:10
        noonScan.line(j).No = ...
            noonScan.line(j).N * exp ( noonScan.line(j).No * noonScan.DT );
    end
end


% STRAY LIGHT
Nstray = 0;
wlStray = 2900;
for j=1:1:4
    if ( noonScan.line(j).wl == wlStray )
        Nstray = Nstray + ((noonScan.line(j).N)/4);
```

```
        wlStray = wlStray + 5;
    else
        break
    end
end


% #CPS BECOMES:
for j=1:1:length(noonScan.line)
    noonScan.line(j).Ncps = noonScan.line(j).No - Nstray;
end


processedScan = noonScan;



*********************************************************************************



function [tailUVI, avg3u] = calcTailUVI(day, endWL)

% READ uvspec out-DATA FILE
% (Used for the calculation of the upper part of the spectrum (the "tail"))

[WL, dir_rad, diff_down, na1, na2, na3, na4 ] = ...
    textread(['halebit/INPoutFiler/day' num2str(day) '.out'],'%f %f %f %f %f %f %f');

for i=1:1:length(WL)

    % Weight factor for action spectrum A
    if (WL(i) <= 298)                          A = 1.0;
    elseif (WL(i) > 298) && (WL(i) <= 328)     A = exp(0.2164*(298 - WL(i)));
    elseif (WL(i) > 328) && (WL(i) <= 400)     A = exp(0.0345*(139 - WL(i)*1.0));
    elseif (WL(i) > 400)                       A = 0.0;
    end
    F(i) = dir_rad(i) + diff_down(i);

    % Tail-part of UVI
    if ( WL(i) > (endWL/10) )
        T(i) = A*F(i);
    end
```

```
    if ( WL(i) == (endWL/10) )
        avg3u = F(i) + F(i-1) + F(i-2);
    end
end
tailUVI = 0.04*trapz(T);



*********************************************************************************



function [UVI] = calcUVI(noonScan, response, endWL, tailUVI, avg3u)

% CALCULATE SPECTRAL IRRADIANCE
for j=1:1:length(noonScan.line)
    if (noonScan.line(j).wl <= endWL)
        noonScan.line(j).spectral_irr = noonScan.line(j).Ncps / response(j).value;
    end
end


% CALCULATING UVI (WITHOUT UPPER PART OF SPECTRUM ("TAIL"))
for j=1:1:length(noonScan.line)
    % Weight factor for action spectrum
    if (noonScan.line(j).wl <= 2980)
        A = 1.0;
    elseif (noonScan.line(j).wl > 2980) && (noonScan.line(j).wl <= 3280)
        A = exp(0.2164*(298 - (noonScan.line(j).wl/10)));
    elseif (noonScan.line(j).wl > 3280) && (noonScan.line(j).wl <= 4000)
        A = exp(0.0345*(139 - (noonScan.line(j).wl/10)*1.0));
    elseif (noonScan.line(j).wl > 4000)
        A = 0.0;
    end
    % UVI without tail-part
    if ( noonScan.line(j).wl <= endWL )
        S(j) = A*noonScan.line(j).spectral_irr;
    end
end
noTailUVI = 0.04*trapz(S)*0.5;

% The upper part of the spectrum ("tail") is calculated for clear
% sky days. Therefore, it needs to be adjusted according to possible
% clouds, aerosols, or similar. This is done here by finding the
```

```
% ratio of the average of the measured irradiance at the three
% largest wavelengths, to the average of the calculated irradiance at
% the same three wavelengths.

% FINDING RATIO (MEASURED DATA)/(UVSPEC) TO MULTIPLY WITH THE "TAIL"
for j=1:1:length(noonScan.line)
    if ( noonScan.line(j).wl == endWL )
        avg3md = noonScan.line(j).spectral_irr ...
                 + noonScan.line(j-2).spectral_irr ...
                 + noonScan.line(j-4).spectral_irr;
    end
end

tailUVI_altered = (avg3md/avg3u)*tailUVI;
UVI = noTailUVI + tailUVI_altered;
```